

Numerical investigation of the wake-diffusion rotor concept



Dmitrij Mordasov

DTU Wind Energy-M-0500
July 2022

Author: Dmitrij Mordasov

DTU Wind Energy-M-0500
July 2022

Title: Numerical investigation of the wake-diffusion rotor concept

Project period:
November 2021 - July 2022

ECTS: 45

Education: Master of Science

Supervisors:

Paul van der Laan
Mads Chr. Baungaard
DTU Wind Energy

Simon Watson
TU Delft

Andreas Knauer
Equinor

Remarks:

This report is submitted as partial fulfillment of the requirements for graduation in the above education at the Technical University of Denmark and Delft University of Technology.

Technical University of Denmark
Department of Wind Energy
Frederiksborgvej 399
4000 Roskilde
Denmark
www.vindenergi.dtu.dk

DTU Wind Energy is a department of the Technical University of Denmark with a unique integration of research, education, innovation and public/private sector consulting in the field of wind energy. Our activities develop new opportunities and technology for the global and Danish exploitation of wind energy. Research focuses on key technical-scientific fields, which are central for the development, innovation and use of wind energy and provides the basis for advanced education at the education.

Abstract

With the growing global utilisation of wind energy, lowering of its levelised cost of energy is pursued. This effort is hindered by wind turbine wakes and their detrimental effects on wind farm profitability. Most currently researched wake mitigation methods are based on wind farm system-level interventions, and there is a research gap on individual wind turbine design wake alleviation measures.

This thesis investigates the wake-diffusion rotor concept, a wind turbine design with an outboard shifted thrust distribution along the blade, and its effects on wake mitigation and power generation in wind farms.

Three wind turbine rotors with equivalent thrust coefficient are modelled as actuator disks in a RANS CFD software PyWakeEllipSys, corresponding to an inboard shifted thrust distribution, a conventional thrust distribution, and an outboard shifted thrust distribution representing the wake-diffusion rotor concept. Investigated scenarios include a single wind turbine and rows of three and ten wind turbines aligned to the inflow. Compared to the baseline case, outboard thrust distribution produces lower wake velocity deficits, increased momentum transfer and increased turbulence generation. The wake-diffusion rotor concept increases the wind farm power generation by 3.8 % and 2.5 % in the three and ten wind turbine row scenarios respectively, with the largest relative gain in wind turbine power of 13.9 % for the second wind turbine in the row. Consecutive wind turbines in the row experience diminishing gains. The inboard shifted thrust distribution had opposite effects for all of these aspects. The benefits in wake mitigation and power generation in wind farms from using the wake-diffusion rotor concept are concluded to come from higher turbulence mixing caused by the outboard shifted thrust distribution. Recommendations on its use for maximum effectiveness are given. Future research could focus on the design implementation of this concept, investigate combinations with other wake mitigation methods and perform parametric wind farm AEP studies.

Acknowledgements

When Maarten Paul van der Laan sat in on my first meeting with another DTU senior researcher, whom I was trying to set up my master's thesis with, I took little notice of the "Oh, I just recently heard this talk at WESC about this interesting concept..." with which he first introduced to me the concept that this thesis is based on. However, the idea had time to marinate in my head, I recognised its ingenuity, and a month later I was reaching out to him to set up this thesis. Some of the best things in life you just sort of stumble into, and I really can not imagine that I could have had anyone better for my main supervisor than Paul. Your expertise in this field, approach to scientific work and kindheartedness made your help and guidance the best I could have asked for. Thanks to you, I enjoyed my master's thesis experience immensely.

My most heartfelt thanks also go to my DTU co-supervisor Mads Christian Baungaard, who listened to the same talk with Paul, explored the concept himself and came up with the idea of turning this concept's investigation into a thesis project in the first place. As a finishing PhD student, you could sympathize with me like no one else, and provided me with invaluable practical advice (not to mention code) - along with those nice coffee talks.

Special thanks to Andreas Knauer, the inventor of the concept investigated in this thesis, who helped me immensely by discussing his inspiration and insights about the concept. I am also grateful to Prof. Dr. Simon Watson, who supervised my thesis project on the TU Delft's side. I would be remiss in not mentioning DTU senior researcher Athanasios Barlas who provided me with some relevant literature for the study.

None of this would be possible without all the support by my family throughout the years. Thank you for letting me truly relax in those rare moments when I came back home, and my dog Vajtik for always giving me a warm welcome.

Last but not least, I have nothing but love for everyone else who was a part of my life during this milestone period of mine. This includes all my roommates, friends and co-workers. Thank you for enduring my rants about debugging and failed CFD simulations.

Glory to God.

Contents

Abstract	i
Acknowledgements	ii
1 Introduction	1
1.1 Motivation	1
1.2 Wake Research	2
1.3 Study Aims	2
1.4 Study's Significance	3
1.5 Assumptions, Scope and Limitations	3
1.6 Thesis Outline	4
2 Wake Diffusion	5
2.1 Wind Turbine Wakes	5
2.2 Wake Modeling	6
2.3 Wake Research Areas	7
2.4 Wake Diffusion	9
3 Method	15
3.1 PyWakeEllipSys and EllipSys3D	15
3.2 DTU 10 MW Reference Wind Turbine	19
3.3 Numerical Grid	22
3.4 Other Parameters, Controlled Variables	26
4 Results and Discussion	29
4.1 Single Wind Turbine Study	29
4.2 Row Study	36
4.3 Design Considerations	43
5 Conclusion	45
A Wake-diffusion Rotor Design	48
A.1 HAWC2S, PyWakeEllipSys Airfoil AD Model	48
A.2 WDR 10 MW Design	49
A.3 Results and Discussion	52
References	57

Nomenclature

Greek Symbols

α	Angle of attack	[deg]
ϵ	Turbulent kinetic energy dissipation	$\text{m}^2 \text{s}^{-3}$
λ	Tip speed ratio	[\cdot]
μ	Dynamic viscosity	$\text{kg m}^{-1} \text{s}^{-1}$
ν	Kinematic viscosity	$\text{m}^2 \text{s}^{-1}$
$\bar{\delta}$	Dimensionless radial distance defined in Subsection 3.1.3	[\cdot]
ρ	Density	kg m^{-3}

Latin Symbols

$\langle U_{AD} \rangle$	Disk averaged velocity	m s^{-1}
C_μ	Turbulence model constant	[\cdot]
C_D	Drag coefficient	[\cdot]
C_L	Lift coefficient	[\cdot]
C_P	Power coefficient	[\cdot]
C_T	Thrust coefficient	[\cdot]
D	Rotor diameter	[m]
f_θ	Dimensionless azimuthal force	[\cdot]
f_T	Dimensionless thrust force	[\cdot]
I	Turbulence intensity	[\cdot]
k	Momentum transfer	s^{-2}
k	Turbulent kinetic energy	$\text{m}^2 \text{s}^{-2}$
P	Power	[W]

R	Rotor radius	[m]
r	Radial distance along rotor blade	[m]
T	Thrust	[N]
U_H	Freestream velocity at hub height	[m s ⁻¹]
x, y, z	Main coordinate system - normal (streamwise), lateral and vertical	[m]

Abbreviations

AD Actuator Disk

AEP Annual Energy Production

BC Boundary Condition

BEM Blade Element Momentum

CFD Computational Fluid Dynamics

DNS Direct Numerical Simulation

DRWT Dual Rotor Wind Turbine

DTU Technical University of Denmark (DAN: Danmarks Tekniske Universitet)

HPC High Performance Computing

LCoE Levelised Cost of Energy

LES Large Eddy Simulation

MRWT Multi Rotor Wind Turbine

NREL National Renewable Energy Laboratory

RANS Reynolds-Averaged Navier Stokes

RWT Reference Wind Turbine

VLM Vortex Lattice Method

WESC Wind Energy Science Conference

WT Wind Turbine

Chapter 1

Introduction

In this Introduction, the general context of this master's thesis project is given in Section 1.1, explaining the significance of wind energy science research today. This is followed by Section 1.2 with a description of the relevant research problems currently being examined in this field, and the research gap present which this study fills. The aims of the study in the form of research questions are given in Section 1.3, followed by the implications that answering these questions would have in the field of wind science energy in Section 1.4. After listing the main assumptions, limitations and scope of this investigation in Section 1.5, this chapter finishes with Section 1.6, outlining the paper's structure.

1.1 Motivation

Not only is there a push for low or no carbon electricity generation technologies in today's energy sector, but the electrification of still heavily fossil-fuel dependent energy sectors, such as heating and transport, coupled with rapidly increasing global energy demand, all increase the appeal of wind energy [1]. Wind energy is a low-cost, clean and proven mainstream energy source, whose role in the energy mix is predicted to grow 15-fold by the year 2050, from being responsible for 5 % of current global energy production to up to 33 % - with a large portion of this possibly being from offshore wind [2, 3]. The science of wind energy is identified to have three *grand challenges* to solve [1], the future research of which could perhaps lead to wind energy even exceeding these current growth estimates [4].

The first two of these identified challenges pertain to 1) *Improved understanding of atmospheric and wind farm flow physics*, and 2) *Aerodynamics, structural dynamics, and offshore wind hydrodynamics of enlarged wind turbines*, with the third one being about electricity grid integration. Wind turbine wakes are a phenomenon in which the energy extraction of a wind turbine affects the flow downstream of the original wind turbine, causing downstream wind turbines in a wind farm to experience this altered flow. The effects of these wakes are mostly negative - they lower wind turbine lifetimes, annual energy production and, overall, the profitability of wind farms [5].

1.2 Wake Research

Considering wind turbine wakes from the point of view of the first challenge, wakes are a key aspect to understanding wind farm flow physics. Taking an aerodynamics perspective, the extraction of energy by wind turbines leaves behind a flow with less kinetic energy to extract - a wake with a velocity deficit, along with a more turbulent structure due to the forces the first wind turbine exerted upon it. The pursuit of understanding and mitigating these wake structures, and thus their effects, spawned large active areas of wake research. The proposed wake mitigation strategies are often on a wind-farm level, and include the fields of layout optimisation, wind farm level control schemes and more.

Researchers tackling the second challenge - that of individual wind turbine design - have a different set of tools and problems. Their main goal could be characterised as, in the big overall picture, trying to optimise the profitability of single wind turbines by trading off power capture against the costs and lifetimes of the individual wind turbine components. However, due to wakes, both power capture and wind turbine lifetimes suffer. The wind turbines they design create the wakes that not only they, but also the researchers focusing on the first challenge, have to solve.

Even though their overlaying objective - developing the field of wind energy - is shared between the two respective challenge areas, there is a research gap present between these two fields of research with different specific problems, goals and methodologies. However, what if, just like Veers et al. [1] calls for, these challenges were combined and solved in a more interdisciplinary manner?

It is this research gap that this study attempts to fill. The 'wake-diffusion rotor concept' takes one of the main tools of the wind turbine designer, the wind turbine blade, and asks - "Can we design this blade to mitigate wakes?" Can the problem, the wind turbine rotor causing the wake in the first place, also be the solution? By changing the blade geometry and thus the aerodynamics of the wake, Knauer [6] in his patent of the wake-diffusion rotor proposes exactly that.

The wake-diffusion rotor has intentionally minimal power extraction near the root of the wind turbine blade, making it suboptimal for wind turbine power generation. However, this design brings about 'ventilation' of the wind flow through the rotor's centre, and lets a jet of high-energy wind, whose kinetic energy was not extracted, into the wake, accelerating wake diffusion. The mitigated wakes, in a wind farm scenario, should theoretically lead to higher power capture of the downstream wind turbines. If balanced well, the small cost in individual wind turbine power generation could pay for itself in increased wind farm power generation [6].

1.3 Study Aims

For the purpose of this study, the wake-diffusion rotor concept is generalised to be a wind turbine, which has the majority of its thrust distribution in the outer radial part of the rotor

- that is outboard, closer to the edges of the blades. Inspired by this novel concept which has gained very little research attention so far, this investigation could be considered to be a feasibility study of the wake-diffusion rotor concept. The research questions could be summarised to be:

- Can shifting the wind turbine's rotor thrust distribution affect its wake dissipation?
- If so, how is this effect achieved?
- What is the order of magnitude of this effect in terms of power capture gains for wind farms?

1.4 Study's Significance

This study hopes to develop several insights for the field of wind energy science.

The evidence generated in this study and its analysis should ascertain the role that rotor thrust distributions, and individual wind turbine design in general, play in wake management. Subsequently, this study should provide a more solid theoretical starting ground for anyone in the field of wind energy science interested in developing this concept further, providing suggestions for future research.

Wake model developers could also use these insights to improve the fidelity of the existing and future wake models, by taking the effects of thrust distributions of modelled wind turbines into account.

If the concept addressed by this study has its feasibility proven and further developed, this could provide wind turbine designers with a new parameter for their design space - the thrust distribution across the wind turbine blades, and thus its effect on the wake. In the long run, this follows in line with a shift from individual wind turbine design to that of wind farm systems, as called for by Veers et al. [1].

1.5 Assumptions, Scope and Limitations

This study will confine itself to the aerodynamics aspects and implications of the wake-diffusion rotor concept only, overlooking structural, dynamic, hydrodynamic and control considerations. Some possible engineering ways of achieving the concept's effects are theoretically explored. However, a design of the wake-diffusion rotor on any level extending above its thrust distribution is not considered to be a deliverable of this study. The aerodynamic scales of motion to be addressed will only be on the microscale level of wind farms, overlooking mesoscale interactions.

The numerical investigation method used - a Reynolds-Averaged Navier Stokes (RANS) based computational fluid dynamics (CFD) solver - is considered high fidelity enough to confirm the validity of identified trends and the order of magnitude of supposed benefits. However, the exact quantification of magnitudes of these benefits in terms of, for example,

power generation, is left for future research.

1.6 Thesis Outline

Following this introduction, Chapter 2 gives the results of a conducted literature study, featuring an overview of the required theoretical background to grasp this study. This is followed by a description of this paper's numerical investigation method in Chapter 3. The results and their analysis, including a discussion, are in Chapter 4. The conclusions made from the investigation and recommendations for further work are given in Chapter 5. Finally, Appendix A contains a design exploration of the wake-diffusion rotor concept.

Chapter 2

Wake Diffusion

This chapter contains theoretical background required for understanding the concept investigated by this thesis, along with the results of the literature review conducted on this topic. It is beyond the scope of this thesis to fully describe the physics of the wake phenomena and its diffusion, along with listing all the possible wake diffusion methods. However, an explanation that should make the reader better understand wakes and the problem posed by them in a wind farm settings is given in Section 2.1. Current state of wake modelling is described in Section 2.2, after which the main wake mitigation research areas are outlined in Section 2.3, to better show the place of the wake-diffusion concept relative to the current state of wake mitigation research. Wake diffusion as a concept is introduced in more detail in Section 2.4, describing the wake-diffusion rotor concept and its inspiration, and includes a review of methods which could be used to achieve it.

2.1 Wind Turbine Wakes

Two main engineering coefficients that non-dimensionalise the capabilities of a wind turbine are used in the science of wind energy.

The first one, power coefficient C_P , usually defined for a whole rotor, is presented in Equation 2.1, and represents the effectiveness of a wind turbine's ability to extract power from the wind [7]. To better understand it, a value of $C_P = 1$ would mean complete extraction of all kinetic energy from the freestream - a physical impossibility. A theoretical limit of $C_{P\max} = 0.593$ was derived, known as the Betz limit [8]. P represents the power generated by the wind turbine, ρ and U_∞ are the freestream wind density, and A represents the wind turbine's rotor area.

$$C_P = \frac{P}{\frac{1}{2}\rho U_\infty^3 A} \quad (2.1)$$

The second coefficient - thrust coefficient C_T - defined for a local thrust dT on an annular element is given by Equation 2.2, in which r is the radial position along the rotor and R its maximum radius [7].

$$C_T = \int_0^R \frac{dT}{\frac{1}{2}\rho U_\infty^2 2\pi r dr} \quad (2.2)$$

The wind turbine, in the simplest terms, generates power by extracting kinetic energy from the freestream. The axial momentum lost in the wake is collected by the wind turbine electrical generator attached to the rotor shaft [5], and is associated with this thrust force due to the work done upon the rotor, so far considered as an actuator disk (AD). Wind turbine wakes are a physical phenomenon, the consequence of this energy extraction process, and the flow's loss of momentum and the forces exerted upon it by the rotor result in a flow with a velocity deficit and increased levels of turbulence. It is common to discern between near and far wake regions, with the near wake (distance up to a few rotor diameters away) being of high interest for research relating to individual wind turbine performance, and the far wake being more relevant to studying the performance of wind farms [9]. The velocity deficit and the increased turbulence negatively affect the downstream wind turbines, easily reducing power output by 10-20 % in wind farms and increasing fatigue loads - which means diminished profits and wind turbine lifetimes [5, 10].

The main parameters that wake losses depend on include inter-turbine spacings (most often given in terms of rotor diameters in the field of wake research), wind speeds, wind direction, turbulence intensity and atmospheric stability [5]. The presence of ground and complex terrain also has its impact, as does the atmospheric stability [9].

On a deeper aerodynamic analysis, the tip vortices shed by the blade's trailing edge, describing helical trajectories immediately downstream of the rotor, have properties such as path, twist angle and strength which impact the behaviour of the wake in the far region. This helix can also be interpreted as a shear layer, separating the slower-moving wake and the outside freestream air [9]. It is the destabilisation and consequent breakdown of this helix that allows for mixing of the wake and the ambient flow, causing further breakdown of the vortices and kinetic energy entrainment in the wake - a process which can be accelerated by higher turbulence [11].

This thesis will concern itself mainly with the wake-diffusion rotor concept, and thus the cause and effect of the wake diffusion mechanism. Thus, the effect of the wake regions' increased turbulence on wind turbine blade structural loads and fatigue damage, along with other aspects, are to be considered outside the scope of the thesis. Where the significance of varying wind turbine blade load distributions will be considered, it will be for the sake of the wake aerodynamics. On top of the wake itself, power capture of wind turbine arrays will be investigated as it is an easily quantifiable parameter which has significant implications on wind farm profitability. There is an applicable rule of thumb that "...each 1 % increase in [wind farm] energy production reduces the LCoE by 1 %" that could be kept in mind [5].

2.2 Wake Modeling

In this relatively early stage of wind farm wake mitigation research, numerical studies dominate the literature due to the associated difficulties and costs of physical measurement campaigns, and will also be the main method employed in this thesis. For a simplified overview of the applied numerical models, consider a scale going from low to high fidelity, starting with engineering models, followed by computational fluid dynamics (CFD) methods ranging from RANS and large eddy simulations (LES) to direct numerical simulations (DNS).

A more thorough treatment of these CFD models is given in Subsection 3.1.1.

Low fidelity engineering models, especially considering the Jensen model [12] and its expanded forms, are the widespread standard used for wake modelling currently. In the Jensen model, the velocity deficit is a function of the upstream wind turbine's overall thrust coefficient C_T - not its distribution. Whilst fine for certain purposes, in applications such as understanding the effect of blade load distributions, active wake control or other wake flow phenomena, more realistic and detailed descriptions of the flow, wake geometry, vorticity and further parameters are required [5, 11]. There are certain parameters - such as the wake dissipation parameter in Jensen's model - that can be tuned to account for the specific characteristics of the wake for the given scenario, one of which can be the wind turbine's thrust distribution. This way, the effect of thrust distribution could be included in these currently used models, even if indirectly.

A number of studies [13–15] remark the importance of thrust distribution on the behaviour of the wake, noting especially the behaviour of the near-wake varying under changing thrust distributions. One important note taken from the study is that in terms of wake velocity and turbulence profiles, cases with higher background turbulence were captured more accurately, thus emphasising the importance of including turbulence effects in wake analysis when running similar simulations. The k - ε turbulence closure model was also found preferable to others for its high agreement with the measured values [13] - whose improved version is used in this study, as described in Subsection 3.1.2.

It could be noted that physical, scaled wind turbine models tested in wind tunnels have been confirmed recently by Wang et al. [16] to produce wakes extremely similar to corresponding full-scaled ones, especially above approximately $x/D = 4$, considering the most usual wake metrics such as the wake deficit, turbulence intensity and shear stresses. However, often due to the facilities available, the researched wake is confined to short distances, usually not extending beyond $x/D = 5$ [17–19], and often much less. Despite this positive assessment, the prohibitive costs and complexities of experimental aerodynamic campaigns explain the research community's preference for numerical studies.

2.3 Wake Research Areas

All the problems associated with wind turbine wakes have lead to the birth and growth of many research areas into alleviating the wake and its effects on wind farms. What follows in this section is an overview of the main wake mitigation methods found in the current relevant literature.

2.3.1 Layout Optimisation

Layout optimisation is currently a large and active field of research, focusing on varying wind farm layouts (position and spacing of wind turbines) in order to maximise power capture through minimising wake losses. An interested reader is pointed to the work of Herbert et al. [20] for a comprehensive overview of the problem of wind farm design optimisation. It should

be noted that power capture is just a single aspect of multidisciplinary optimisation in this area, as factors such as civil engineering infrastructure, electrical interconnections and more often play part in the optimisation problem.

2.3.2 Sector Management

Sector management is a simple approach taken in wind farms with severe wake effects, consisting of shutting down wind turbines in certain problematic conditions (e.g. a combination of a high wind speed and a certain direction), preventing excessive fatigue loading and vibration issues [5]. Increasing wind farm yields is also possible, as shown by Haces-Fernandez et al. [21]. With more understanding of the wake effects for a given scenario, the strategy's negative impact on energy production can be lessened by for example derating the upstream wind turbines only, which introduces the next wake mitigation means.

2.3.3 Axial Induction Control

Axial induction control is a wake management concept that tries to reduce the velocity deficits of the wakes impacting downstream wind turbines by varying the induction factor of upstream wind turbines, generally decreasing the production of the upstream wind turbines whilst resulting in an overall power production increase over a wind farm [11]. However, whilst the technique seems to be mainly based around lowering the wind turbine's thrust, an opposite approach of operating the wind turbines at higher thrust is explored by Martínez et al. [15] (highly reminiscent of the wake-diffusion rotor concept, treated in more detail in Subsection 2.4.2). This research area seems to lack in high-fidelity simulations (studies are mostly using engineering wake models rather than CFD) and field tests, along with a consensus on the best practices of its implementation, but may have the potential to provide single-digit percentage increases in wind farm annual energy production (AEP) [11].

2.3.4 Wake Steering (Yaw Control)

Wake steering through yaw control tries to maximise wind turbine array power production through yawing upstream wind turbines, and thus 'steering' the produced wake, once again leading to increased power production of downstream turbines through either deflecting the wakes or forcing their interaction. Appears to hold more promise than axial induction control for power maximisation, due to higher quality of research at the present time [11].

2.3.5 Dynamic Induction Control

Dynamic induction control is a very recent wake management technique, in which a dynamic set point for wind turbines is used in order to manipulate the wake instabilities and have them interact in order to accelerate vorticity decay, increase turbulent mixing and thus speed up wake recovery (well explained in Houck and Cowen [22], and investigated by Munters and Mayers [23, 24]). Whilst there seems to be a large potential for power capture gain, there are concerns over additional caused loads, and much more further research is required (especially) for implementation in wind farms, but remains a possible future wake mitigation strategy [11].

In VerHulst and Menevau [25], a synthetic vertical forcing is applied to an AD model in a LES simulation, conceptually mimicking "...the effects of, e.g., rotor tilting or fast-acting blade control schemes, which could generate net thrust components in the vertical directions by suitably-controlled angle-dependent pitch variations." The conclusion of the study was that a significant increase in the wake kinetic energy entrainment could be gained thanks to this unconventional actuator disk forcing, increasing power extraction [25].

An example of the above may be seen in a relatively novel investigation of Frederik et al. [26], increasing downstream wake mixing by disturbing the wake through dynamic individual pitch control - that is, actuating pitch servos on individual wind turbine blades. The study's results affirm this to be a viable approach for increasing power production in wind farms, with possibly lower variations in power, thrust and thus loading than dynamic induction control.

2.3.6 External Wind Farm Devices

In what may be the most avant-garde way to mitigate wake effects found in current literature so far, an investigation by Bader et al. [27] claims that placing external devices (supported stationary structures, mostly based on airfoils) in the wakes of wind turbines can have significant wake mitigation potential. These could displace the upstream turbine's wake away from the one downstream, or in some cases even accelerate the wind impacting the downstream turbine. This could be considered as an interesting take on wake steering through external means.

2.4 Wake Diffusion

In this section, the wake-diffusion rotor concept will be introduced, along with a selection of literature pertaining to it. The investigated concept could be considered quite novel, and it has garnered little attention in the current research community so far, such that evidence for the concept's working mechanism and possible means of achieving or utilising it must be extracted from other insights in relevant fields. Many of these concepts have been found in NREL's multidisciplinary literature review 'Investigation of Innovative Rotor Concepts for the Big Adaptive Rotor Project', conducted by Johnson et al. [28].

2.4.1 The Wake-diffusion Rotor Concept

The wake-diffusion rotor concept, as described in the patent by Knauer [6], who developed it while working as a specialist in Equinor, is the inspiration that lead to the investigation in this thesis. The main idea behind the concept is that a wind turbine blade, commonly optimised for power capture (coupled with structural, aeroelastic and economic considerations), could rather be designed to produce a wind turbine wake that would dissipate more quickly than for the conventional design. Whilst there would be a small loss in the power capture of an individual wind turbine (as it would no longer be optimised for power capture), on a

wind-farm level, the faster-dissipating wake would lead to consecutive downstream wind turbines to be able to extract more energy from the flow, leading to higher overall AEP.

This rotor blade geometry would, at the root section (where the blade is often thicker and with higher chord length due to structural reasons), ‘ventilate’ the incoming wind - the root section is no longer designed for optimum power extraction as in conventional design - extracting less kinetic energy around the centre of the rotor plane and thus creating a jet of fast flowing air in the centre of the wake. The outer part of the blades remains shaped for maximum power extraction. This creates a load distribution on the rotor that produces a wake in which the additional kinetic energy from the ventilated inner section produces additional shear with the helical vortices shed by the wake, increasing turbulence, promoting mixing of the wake and thus effectively mitigating it more quickly. The concept was first successfully tested numerically, later followed by physical wind tunnel tests (on a 3-WT model row) [6].

This concept, through personal correspondence with Knauer, was found to be inspired by older research on bluff-body drag reduction as shown in Suryanarayana et al. [29], in which a hole was made through the centre of the sphere at its stagnation point. The ventilation provided by this has reportedly reduced the drag of the sphere by more than half, adding additional mass, momentum and energy to the near wake, the width of which was reported to be constantly changing (more than for a solid sphere), implying increased turbulence and thus mixing.

2.4.2 Wind Turbine Rotors Under High Thrust

A most relevant proposed model can be found in Martínez-Tossas et al. [15], which investigates the effect of increasing the thrust coefficient C_T of the wind turbine to very high levels. Increased wake turbulence and accelerated wake recovery is attributed to the higher C_T operation, and the distribution of this thrust along the blade was not neglected. Three ways of achieving the high $C_T = 1.3$ in this numerical investigation are utilised - varying (1) turbine rotations per minute (RPM), (2) pitch or (3) prescribing constant C_T along the blade. Varying turbine RPM has been found to "...generate the largest difference of loading throughout the blade. This difference comes from the higher relative velocities from increasing the rotational speed." [15] The effect of this was a strongly outboard-shifted thrust distribution along the wind turbine blade, resulting in the largest Reynolds stress production, and faster wake dissipation than the other two operational modes with the same C_T . This further supports the notion behind the Equinor blade’s load distribution.

2.4.3 Dual-Rotor Wind Turbine

Dual-rotor wind turbines (DRWTs) have already been found to theoretically surpass the well-known Betz limit of 59.3 % back in 1986 by Newman [30], showing that a DRWT of an equivalent size to a conventional rotor can achieve a larger power coefficient C_P , allowing up to 64 % kinetic energy capture from the freestream wind. The analysis of the wake of

such a DRWT is one of the main goals of the investigation by Rosenberg et al. [31], in which a DRWT is designed with both increased capture and faster wake recovery in mind. A LES simulation of this concept does lead to an increased power generation (of about 4.6 %), yet does not find any conclusive evidence pertaining to wake recovery. However, the simulation was run only for long enough for the wake to convect itself roughly once down the computational domain ($x/D = 8$ long), and wake field variables are averaged over an even shorter period of time, likely leading to a statistically unconverged solution that suggests insufficiency of data for wake analysis purposes. This is highly unfortunate, as the higher energy extraction in the middle of the rotor area near the root could have provided some insight, being an ‘opposite’ design modification compared to that of the wake-diffusion rotor concept.

2.4.4 Multi-Rotor Wind Turbine

It could be argued that a multi-rotor wind turbine (MRWT) design mimics the proposed wake diffusion mechanism by having a ‘hole’ in its middle (near the root), where it lets the freestream flow through, thus emulating a single rotor with a strongly varying load distribution such as the Equinor concept. Faster wake recovery for a MRWT is found in investigations of van der Laan et al. [32] (field measurement) and of Ghaisas et al. [33] (LES). A prompt towards discerning the physical mechanism behind the faster wake recovery is made in the latter, and it is likely that MRWTs share some similarity with the wake-diffusion rotor concept in this case, as discussed in Subsection 4.2.3.

2.4.5 Blade Geometry

In Kelley et al. [34], there are some very interesting insights found in a vortex-lattice method (VLM) investigation of the wake of two different blade designs, having an identical integrated C_T over the blade yet different blade loads, with blade B being unloaded in the last 25 % of the blade span near the tip. The wake produced by (conventional) blade A recovers less quickly in the near wake (before $x/D = 5$) than the power-suboptimal blade B, and this concludes that “... larger spanwise gradients of bound circulation and larger induced angular velocity exhibit shorter and faster mixing far-wakes...”, with evidence that it is not vertical momentum transfer as much as the angular momentum of the wake leading to this faster breakdown [34]. It should be noted that the velocity deficit of the more-loaded blade A does become lower than that of B, but only in the far wake above $x/D = 5$. Design B wake width decreases faster than that of design A. It is also interesting that this loading is basically the opposite of the one in wake-diffusion rotor concept as presented by Knauer [6]. The conclusions of this study are slightly questionable, as the VLM simulation was ran for such a short time that it would have allowed for only roughly two passes of an air particle through the wake domain, once again likely leading to statistically unconverged results (as in the DRWT LES study mentioned before [31]).

This design relying on the decreased wake velocity deficit in the distance not so far from the original wind turbine downstream has also been patented by the same Kelley et al. [35], with

much reasoning borrowed from the previous work [34]. It is interesting how both this and the design by Knauer, whilst almost directly conflicting with how the thrust distribution for wake diffusion is spread across the wind turbine blade, are both believed by their respective authors to increase wind farm yields through the wake diffusion mechanism. Kelley et al. attribute the said wake diffusion to increased tangential velocity or angular momentum stemming from the increased inboard blade loading, leading to larger axial velocity gradients in the near wake assumed to affect the wake's stability. Do note that since the effect from the given load distribution is confined to a shorter distance downstream, it is also the idea of the patent to place the wind turbines in this region as well. However, as previously mentioned, the insufficiency of the data in the original study [34] do raise doubts as to the conclusions pertaining to the optimum thrust distribution for faster wake recovery. The investigation present in this thesis can clarify this issue.

Moving on, the relatively recent study by Moghadassian and Sharma [36] shows great support for the wake-diffusion rotor concept. In it, an inverse design approach is taken, varying rotor geometry (chord length, twist) of wind turbines in order to optimise wind farm power capture. Using a RANS AD model, it achieves about a 6.5 % C_P increase (averaged over the wind turbine array) in a 10-WT row. Analysing the farm-optimised blade geometry, the main changes are made for the blade's chord, in which its distribution changes such that the chord decreases (compared to baseline NREL 5MW RWT) at the root, and increases near the tip. The discussion in the study closely follows the reasoning of the wake-diffusion rotor concept, mentioning the passing of high-momentum air into the wake to promote wake diffusion and thus reduce the velocity deficit at downstream wind turbines.

A similar optimisation investigation is done by Allen et al. [37]. In one of the case studies present, a blade chord distribution is optimised for the sake of increasing the entrainment of kinetic energy for a single wind turbine, leading to the fastest wake re-energisation. This has resulted, once again, in a chord distribution where the blade chord at the root was decreased and increased near the tip. It should be noted that in this study, while the increased thrust lead to higher velocity deficits in the near wake, the entrained kinetic energy resulted in greater wake recovery (beyond $x/D = 2$) downstream.

A bioinspired swept blade design was recently experimentally investigated by Nafi et al. [19], leading to a conclusion that such a design could be beneficial for use in wind farms. The investigated blade design produced results which showed a significantly lower momentum deficit and turbulent kinetic energy production compared to a conventional, straight wind turbine blade. The swept design seems to benefit from reduced load fluctuations and lower drag from a higher lift-to-drag ratio, bringing structural benefits, at the cost of possibly inhibiting faster wake recovery due to the relatively low turbulent nature of its wake.

Yang et al. [14] conducted an LES investigation on the effect of spanwise load distribution of two varying blade designs of equivalent C_T . A conventional, power-optimised design A is compared to design B in which the loads are shifted closer towards the root of the blade, and it is found that the (power-suboptimal) design B has slower wake recovery than design A. Thus, as blade B has opposite thrust distribution, it can be considered to support the feasibility of the wake-diffusion rotor concept and its outboard thrust distribution.

2.4.6 Blade Tip Treatment

In Tobin et al. [17] an increase in C_P and C_T (8.2 % and 15.0 % respectively) on a scaled wind turbine model in a wind tunnel test is achieved through the implementation of winglets on a turbine blade, leading to increased mean shear in the near wake, and increased turbulence and Reynolds stresses in the far wake. However, due to the theoretical treatment in that study that uses the Jensen wake model [12] (which does not take the distribution of the C_T increase into account), the power capture increase is argued to come thanks to the increase in C_P at the cost of the increase in C_T . Furthermore, whilst they found increased mean shear in the near wake, and thus in the far wake a higher turbulence intensity and Reynolds stresses, the wingletted turbine still leads to higher wake deficits in the measured regions (last one between $x/D = 4$ and about $x/D = 5.2$), most likely explainable once again by the overall increase in C_T and thus momentum extraction from the flow rather than just a change in its distribution over the wind turbine blade.

The effects of winglets and blade serrations on wake dissipation were investigated by Klimchenko and Jones [18]. The investigation focused on wing tip vortices, assuming that the blade tip treatments could affect them, reducing their strength and accelerating their decay in order to encourage wake mixing. Limited quantitative treatment was made for only up to $x/D = 1.8$ (physical, scaled wind turbine model in wind tunnel), which produced no discernible effect on the wake deficit caused by the blade tip treatments. However, a qualitative difference in tip vortex structure was noticed, prompting possible further investigation, especially beyond the very-near wake region.

2.4.7 Flow Devices

A Gurney flap is a passive flow device that is able to increase individual wind turbine power capture through controlling the flow over the airfoil, reducing flow separation and thus leading to improved aerodynamic performance. A numerical investigation is conducted by Zhang et al. [38], in which two Gurney flap configurations are applied near the root of the blade, and it should be noted that these devices have significantly altered the local C_T in the blade, which could show promise as a potential design decision that could be tried to produce the wake diffusion effect through altering blade thrust distribution. Analysis of wake behaviour was not present in the study.

Whilst active wind turbine flaps seem to be mainly investigated for their potential in blade load alleviation, they are also found to be able to increase wind turbine AEP by up to 1 % by McWilliam et al. [39]. Trailing edge flaps and their effect on wake characteristics on top of power capture are investigated by (a different) Zhang et al. [40]. Deflecting the trailing edge flaps near the tip of the blade has resulted in increased velocity deficits in the wake, as per their RANS simulation. Negative deflections of the trailing edge flap (leading to decrease in camber of the airfoil shape of the blade, reducing the load and thus overall C_T) have lead to increased wake recovery. Another similarity of note is that positive deflection (higher

loading) did result in increased wake recovery, but only at $x/D = 1, 12, 14, 16$ downstream, or the very near and far wake. These results suggest that, if not keeping the overall C_T of the blade constant, the benefits of increasing it on the blade may lead to inhibition of wake recovery even though a more outboard thrust distribution is used (such as in Tobin et al. [17]).

The fact that the active flaps may increase or decrease the blade loads show the potential of the concept in wake diffusion applications as well by the author's opinion, supported by the findings of VerHulst and Menevau [25].

2.4.8 Combined Approaches

Combined approaches, due to the lack of best practices or maturity of the single wake mitigation methods, are still in a very early stage of research, but potentially can hold some promise by alleviating the issues present in their component approaches. It is situated at the end of this chapter due to the mentions of previously treated wake mitigation methods.

A combined approach popular in current research among the control solutions is the combination of axial induction control and wake steering, the state of which is reviewed by Houck [11].

Hardware solutions can be complemented with control wake mitigation concepts, such as in the case of using yaw steering with multi-rotor wind turbines in Speakman [41].

Of note should be the third case study in Allen et al. [37], in which a blade design optimisation was performed that would balance wake deflection (yaw steering), kinetic energy entrainment (leading to faster wake re-energisation) and individual turbine power output, leading to the largest power capture of a two wind turbine configuration. The resulting blade design kept its chord distribution at the root, and increased near the tip, thus increasing the outboard thrust on the blade.

Stanley and Ning [42], in an attempt to optimise wind farm yields, couple wind turbine design with layout optimisation, using nonhomogeneous wind turbine types (more than one wind turbine type in a wind farm). The optimisation study explores varying hub heights, rotor diameters, turbine ratings, tower diameters, tower shell thicknesses and blade chord-and-twist distributions coupled with wind farm layout in order to maximise the wind farm's cost of energy. The superiority of this approach to sequentially optimised turbine design is discovered, and a relevant conclusion is that small wind farms have the largest benefits from coupled optimisation. Unfortunately, the chord-and-twist distributions in the study were optimised for the purpose of limiting the blade mass in this study only, hence neglecting the possible wake-diffusion effect. Moghadassian and Sharma [36] also argued for the increased wind farm power capture through varying wind turbine blades across wind turbines in.

Chapter 3

Method

In this chapter, the methodology of this numerical investigation of the wake-diffusion rotor concept is given. This begins in Section 3.1 with a description of the simulation software and the models used. Section 3.2 follows with a description of the baseline wind turbine used in this study, and the modelling approach taken for it and for the wake-diffusion rotor. The process and results of a grid independence study are presented in Section 3.3, and the chapter concludes by giving an overview of controlled variables, assumptions and such information in Section 3.4.

3.1 PyWakeEllipSys and EllipSys3D

PyWakeEllipSys is the CFD software package to be used for the numerical investigation. It combines a RANS based wind farm flow model with PyWake, an open source AEP calculator, with the RANS model being based on the general purpose flow solver EllipSys3D. This is a Fortran/MPI based closed source licensed software, the development of which was initiated at DTU by Sørensen [43] and Michelsen [44] and is continued by the DTU Wind Energy. Python is the programming language used to interact with PyWakeEllipSys, and the simulations are computed on the central DTU HPC cluster.

3.1.1 RANS Modeling

Fluid motion can be described by the Navier-Stokes equations, which mathematically express the laws of conservation of mass (Equation 3.1, assuming incompressible flow) and momentum (Equation 3.2).

$$\frac{\partial u_i}{\partial x_i} = 0 \quad (3.1)$$

$$\frac{\partial u_i}{\partial t} + u_j \frac{\partial u_i}{\partial x_j} = -\frac{1}{\rho} \frac{\partial p}{\partial x_i} + \nu \frac{\partial^2 u_i}{\partial x_j \partial x_j} + f_i \quad (3.2)$$

Where, using Einstein notation, the field variables u , p , ν and f represent the velocity, pressure, kinematic viscosity ($\nu = \mu/\rho$, where μ and ρ are the fluid dynamic viscosity and density respectively) and body forces of the flow field respectively.

No analytical solutions are known for the Navier-Stokes equations, due to the pressure-velocity coupling (linear dependence of pressure on velocity and vice versa), which makes the partial differential equation nonlinear. With certain simplifications, a general solution can be arrived at, yet these would possibly make the result unrealistic for the given flow scenario, such as a laminar flow assumption. When the inertia of a laminar flow becomes sufficiently large such that viscous and other stabilising forces can no longer restrain small irregularities in the flow field, the perturbations grow into highly convoluted, unsteady, seemingly chaotic ‘eddy’ flow structures in a phenomenon we call ‘turbulence’.

Numerical solutions of the Navier-Stokes equations are possible through DNS, yet computationally expensive. This is due to the fact that without modeling the turbulence, DNS models need to resolve the whole range of spatial and temporal scales of turbulence, requiring very fine numerical grids, small time steps, and large memory storage requirements. For the Reynolds number orders encountered in wind turbine wake modeling, the computational cost is prohibitively high.

LES is a popular type of turbulence models in research, which makes these simulations computationally feasible by skipping the resolution of the smallest flow length scales through filtering. Used for its high fidelity, there is still a large computational cost associated with this model.

RANS turbulence models, compared to LES, save on computational cost by roughly three orders of magnitude [45]. For studying purely single wake characteristics, the higher fidelity LES model could be argued for, yet RANS was chosen due to the wind turbine array analyses planned in the initial scope of the thesis project, which would have proved prohibitively computationally expensive. RANS models work on the basis of applying a Reynolds decomposition - which describes the flow field as a combination of its mean and fluctuating part (e.g. $u_i = \bar{U}_i + u'_i$), thus ‘time-averaging’ the flow field.

This procedure, through the non-linearity of the convective term in the momentum equations, produces a Reynolds stress tensor (consisting of six new Reynolds stress terms) in the RANS equation:

$$\frac{\partial \bar{u}_i}{\partial t} + \bar{u}_j \frac{\partial \bar{u}_i}{\partial x_j} = -\frac{1}{\rho} \frac{\partial \bar{p}_i}{\partial x_i} + \nu \frac{\partial^2 \bar{u}_i}{\partial x_j \partial x_j} - \frac{\partial \bar{u}'_i \bar{u}'_j}{\partial x_j} + f_i \quad (3.3)$$

In which $\bar{u}'_i \bar{u}'_j$ are the Reynolds stresses, and the viscous term can be essentially ignored for high Reynolds number flows such as the one in this study.

Just like normal materials have a property of viscosity, turbulence can be modelled by assuming that in flows, the turbulent momentum transfers are similar to molecular ones - done by introducing a ν_T ‘eddy viscosity’ term using the Boussinesq hypothesis [46]:

$$\overline{u'_i u'_j} = \frac{2}{3} k \delta_{ij} - \nu_T \left(\frac{\partial U_i}{\partial x_j} + \frac{\partial U_j}{\partial x_i} \right) \quad (3.4)$$

This helps model the U -momentum Reynolds stresses, (normal, $\overline{u' u'}$) lateral ($\overline{u' v'}$ and vertical $\overline{u' w'}$) the analysis of which (and especially their gradients), can help describe momentum transport in the given flow scenario.

3.1.2 k - ε - f_P Turbulence Model

Assuming an existence of an ‘eddy viscosity’ ν_T as a property of the flow and then using the Boussinesq assumption (see Equation 3.4), along with a turbulence model for the eddy viscosity, the turbulence closure problem of the Navier-Stokes equation is solved and a solution to the given flow can be calculated. The particular turbulence model to be used in this investigation is the k - ε - f_P model, a modified k - ε model "...better suited for simulating wake effects on the power production of wind farms" which is outlined in van der Laan [45]. By directly using a correcting scalar function f_P as in Equation 3.5, the eddy viscosity in flow regions of high velocity gradients is dampened where it would usually be overpredicted by the standard k - ε model - that is, usually at the wake boundary, leading to an underpredicted velocity deficit [47].

$$\nu_T = C_\mu f_P \frac{k^2}{\varepsilon} \quad (3.5)$$

3.1.3 Actuator Disk Model

In CFD simulations of wind farms (both RANS and LES), the resolution of the entire blade geometry is not too feasible if one wants realistic computation times, as that would require the resolution of complex, small-scale flows across the blade. Hence, methods that insert the body forces f_i that appropriately describe the wind turbine loading such actuator disk, line and surface approaches exist [5]. All of these methods apply body forces in the flow solver by first estimating the blade forces based on the specific model used and then redistributing these in the computational domain.

The AD model, acting as a momentum source term in the RANS equation used by PyWakeEllipSys uses a disk polar coordinate grid, which is coupled with the main flow domain grid as described in Réthoré et al. [48], with the forces being allocated as per Troldborg et al. [49].

Joukowsky Rotor

Such an AD model, so called ‘Joukowsky’¹ AD as described in Sørensen et al. [50], is used in this investigation. It is an analytical AD model for axial and tangential forces based on a constant circulation assumption, corresponding to a Joukowsky rotor, modified with tip and root corrections $F(\chi)$ and $g(\chi)$, where $\chi = r/R$. The dimensionless thrust and azimuthal surface forces f_T and f_θ are written as:

$$\frac{f_T}{\rho U_0^2} = q_0 \frac{gF}{\chi} \left(\lambda \chi + \frac{1}{2} q_0 \frac{gF}{\chi} \right) \quad (3.6)$$

$$\frac{f_\theta}{\rho U_0^2} = \frac{u_D}{U_H} q_0 \frac{gF}{\chi} \quad (3.7)$$

Where U_0 and $u_D(r)$ are the inflow and axial velocity in the plane of the rotor respectively, λ is the tip speed ratio, and q_0 is the dimensionless reference circulation (see Equation 3.10). Axial loading is integrated over the actuator disk for thrust T , and the associated thrust coefficient C_T can be expressed as:

$$T = \int_{AD} f_T dA = \int_0^R f_T 2\pi r dr = 2\pi R^2 \int_0^1 \chi f_T d\chi \quad (3.8)$$

$$C_T = \frac{T}{\frac{1}{2} \rho \pi R^2 U_0^2} = \frac{4}{\rho U_0^2} \int_0^1 \chi f_T d\chi = 4q_0 \lambda \int_0^1 gF \chi d\chi + 2q_0^2 \int_0^1 \frac{g^2 F^2}{\chi} d\chi \quad (3.9)$$

As thrust coefficient and tip speed ratio are given, and writing Equation 3.9 as $C_T = 2a_1 q_0 + 4\lambda a_2 q_0$, the reference circulation is determined from Equation 3.10. Equations 3.6 and 3.7 are used to compute the AD force distributions.

$$q_0 = \frac{\sqrt{16\lambda^2 a_2^2 + 8a_1 C_T} - 4\lambda a_2}{4a_1} \quad (3.10)$$

The classical Prandtl tip correction is used, as per Betz [8]:

$$F = \frac{2}{\pi} \arccos \left[-\frac{N_b}{2} \sqrt{1 + \lambda^2} \cdot (1 - \chi) \right] \quad (3.11)$$

In which $N_b = 3$ is the number of blades. A vortex core of size δ is used in this model in order to account for the influence of the hub and the inner non-lifting part of the rotor, with the corresponding expression for the root correction:

$$g = 1 - \exp \left[-a \left(\frac{\chi}{\delta} \right)^b \right] \quad (3.12)$$

¹The author, as an ethnic Russian, would like to note that the most proper transliteration is ‘Zhukovsky’.

Where a and b are root correction coefficients, and $\bar{\delta} = \delta/R$ is the dimensionless radial distance to the point of maximum azimuthal velocity, typically corresponding to the point where the lifting surface of the rotor starts. It is through the manipulation of the vortex core size δ that varying thrust distributions over the blade are achieved, with $\bar{\delta}$ being an input variable into the AD forcing model in PyWakeEllipSys. The thrust distribution, once prescribed, remains fixed, and the azimuthal force distribution varies depending on the local axial velocity in the rotor plane [50]. C_T , C_P and λ curves are an input into PyWakeEllipSys, see Section 3.2.

An implicit expression $(a \cdot b + 1) \exp(-a) = a$ between the coefficients a and b is derived from the fact that the tip correction is approximately unity at the root, and by default, corresponding values of $b = 4$ and $a = 2.335$ are used due to their fit to the empirical nature of the azimuthal velocity distribution at the rotor root [50].

For the purposes of the thesis, a variant of this AD forcing method will be used that takes into account the tangential force (that induces wake rotation), along with wind shear and veer effects. This is often disregarded in wind farm AEP calculations to save on computational cost due to the negligible effect on the power deficit in neutral conditions [51]. Combined effects of shear and wake rotation are expected to lead to an asymmetric wake deficit.

3.1.4 AD Model Control Method

An AD control method to model interacting wind turbines is employed by PyWakeEllipSys [52]. The dependence on inflow wind speed and wind turbine size are removed in favour of ambient (inflow) turbulence intensity, prescribed stability and the wind turbine thrust coefficient distribution, resulting in a reduction of computational resources needed for AEP calculations.

In this case, a $C_T^* - \langle U_{AD} \rangle$ look-up table is made, in which C_T^* is a scaling coefficient and a function of $\langle U_{AD} \rangle$, the local velocity averaged over the AD disk. This is based on a calibration procedure involving single wake simulations, where each simulation has a physically different inflow (corresponding to freestream velocities between the wind turbine cut-in and cut-out, uniformly spaced by 1 m s^{-1}). The total AD forces of these simulations are prescribed and $\langle U_{AD} \rangle$ is extracted from the converged solutions [51].

3.2 DTU 10 MW Reference Wind Turbine

The wind turbine used as a baseline for the investigation in this thesis is the DTU 10 MW Reference Wind Turbine (DTU 10MW RWT), as described in Bak et al. [53]. This was chosen due to the relevancy of the design towards the current industry trends of offshore wind farms [3]. There are C_T , C_P and λ curves of this wind turbine available (closed source), required as input into the PyWakeEllipSys model, along with freely available HAWC2S wind turbine input data² (see Section A.1). The rotor's diameter D is equal to 178.3 m, and it has

²GitLab DTU 10 MW RWT project page, <https://rwt.windenergy.dtu.dk/dtu10mw/dtu-10mw-rwt>.

a hub height $z_H = 119$ m.

3.2.1 Joukowsky AD Model $\bar{\delta}$ Tuning

In Figure 3.1 it can be seen that with increasing the $\bar{\delta}$ parameter shifts the thrust distribution³ over the wind turbine blade more towards the tip, decreasing the loads experienced at the rotor root. This effect can be viewed as increasing the ‘ventilation’ present in the centre of the rotor disk, letting more air through and thus injecting a stream of energised air into the wind turbine wake.

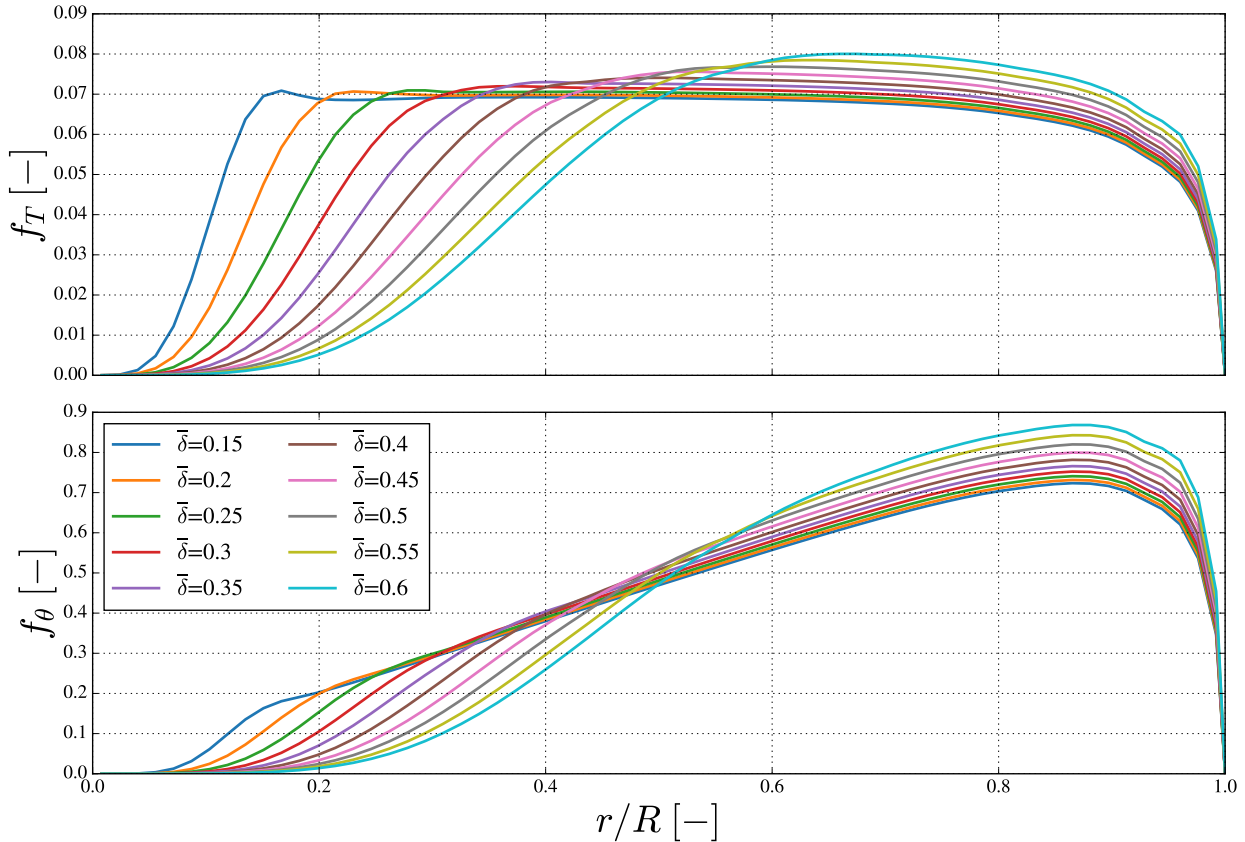


Figure 3.1: Dimensionless thrust and azimuthal force distributions for the AD Joukowsky model of varying $\bar{\delta}$.

³Non-dimensionalised by multiplying the force per unit length, extracted from the simulation, by $1/\rho R U_H^2$.

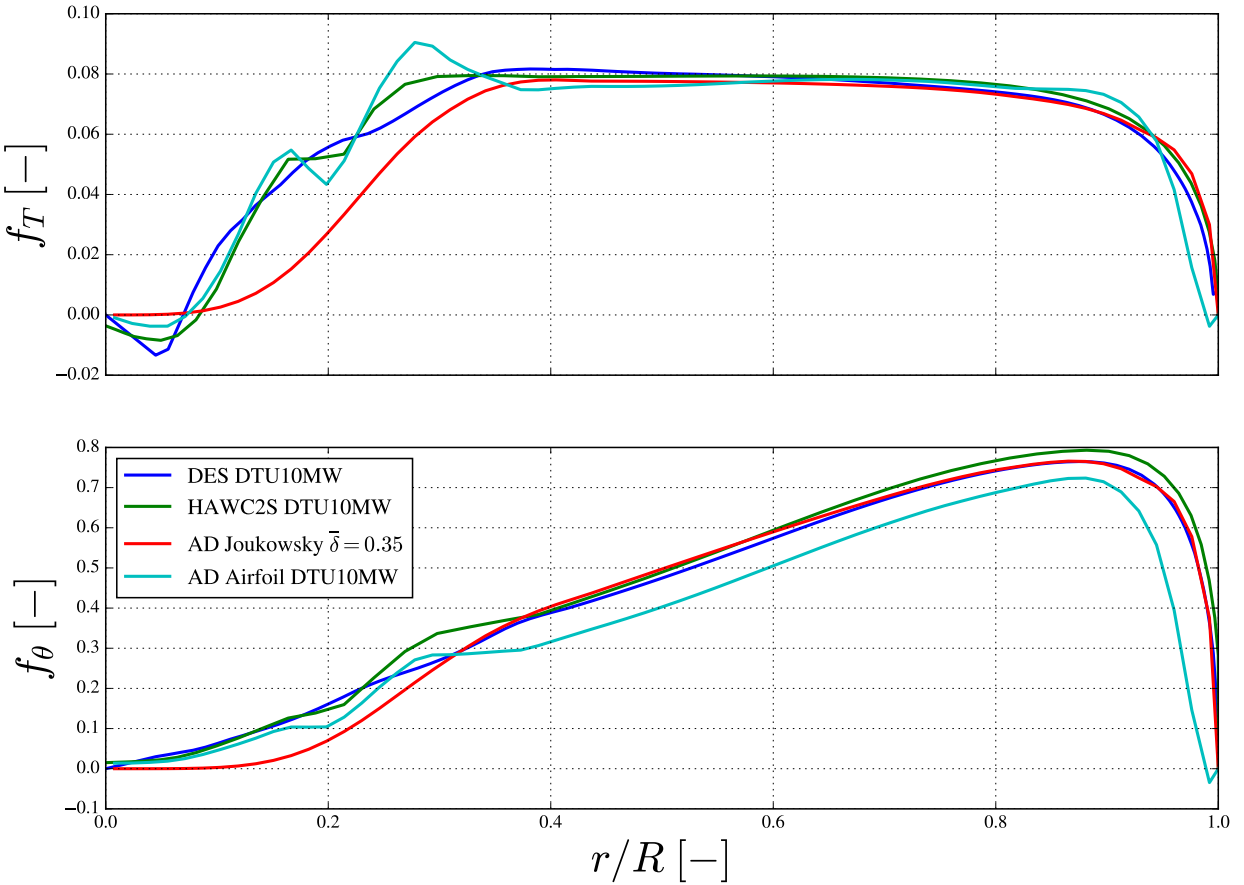


Figure 3.2: Dimensionless thrust and azimuthal force distributions along the blade for various numerical model representations of the DTU10MW.

In Figure 3.2, a Joukowsky AD model with $\bar{\delta} = 0.35$ is found to empirically fit the detached eddy simulation (DES) data and the airfoil AD (see Section A.1) the most, and is to be considered the baseline for the Joukowsky rotor. It should be noted that this is the specific case for the chosen DTU 10MW RWT, as, for example, the NREL 5-MW RWT (another very popular reference wind turbine used in research, described in Jonkman et al. [54]) was found to have a closer fit with $\bar{\delta} = 0.25$ by the author, and can be seen in Appendix A2 in work of Baungaard [55]. The DES data was obtained from the DTU 10MW RWT project page⁴. A small limitation of the Joukowsky AD model is the lack of representation of the nacelle in its force distributions, which could lead to lower wake deficits at the centre of the wake [45]. A minimum value of $\bar{\delta} = 0.15$ is chosen as most current conventional wind turbine rotors do not have high thrust in the root section, often consisting of a thick cylindrical section for structural and aeroelastic reasons. A maximum value of $\bar{\delta} = 0.60$ is chosen, as it is difficult to conceive a wind turbine blade with thrust spread even more outward than this - once again due to structural and aeroelastic considerations that would arrive from the blade experiencing such high forces this far from the root.

Finally, the effect of changing root correction coefficients a and b (see Equation 3.12) was

⁴See footnote 2.

found to have changed the gradients of thrust and azimuthal force distributions near their inflection points, and the aforementioned values of $a = 2.335$ and $b = 4.0$ were kept due to the best fit to the modelled wind turbine.

3.3 Numerical Grid

The numerical grid to be used in this study is Cartesian, with uniform roughness and elevation reminiscent of offshore wind farm conditions (see Subsection 3.4.1). It can be described to consist mainly of two parts - a general, coarser flow domain, and a finer wake domain in the vicinity of the wind turbines, which are represented by actuator disks (see Subsection 3.1.3).

A grid independence study is performed in order to arrive at converged solutions in PyWakeEllipSys of acceptable accuracy, whilst trading off for computational expense of the simulations based on the level of grid fineness. With EllipSys3D being established software in wind energy research at DTU, the author is thankful to have access to pre-existing body of practical knowledge on the utilisation of the software for research purposes. This has provided a good starting point, and reduced the number of required iterations ran in order to begin the studies which are the main focus of this thesis [56].

A default flow domain grid with a cell expansion ratio of 1.2 is used in this investigation, which takes up about 80 – 90 % of the whole numerical grid (situated around the finer wake domain, which contains the wind turbine and its wake). Since this investigation focuses on the effect of varying force distributions along the blade and the effects on the wake, the wake and the AD grids are considered to be important for the accurate resolution of wake behaviour. Preliminary simulations have indeed found these to have a large effect on the measured values of power and the velocity deficit in the wake, hence a grid study on these parameters is undertaken. For the velocity deficit, the velocity across an AD grid of the same size as the wind turbine rotor at $x/D = 5$ (see Subsection 3.4.2) was integrated and averaged over the surface, to be compared to the inflow wind speed.

Power P and wake velocity deficit ($\langle U_{AD}/U_H \rangle$ are probed at $x/D = 5$) of the DTU 10 MW RWT using the AD airfoil model (see Section A.1), using the simulation parameters described in this Chapter 3. These are used to calculate relative power and wake velocity deficit errors⁵ δ_P and δ_U respectively.

3.3.1 Wake Domain Grid Spacing

In a wake domain grid study performed in previous research [45], also using PyWakeEllipSys, eight cells per rotor diameter were found to be sufficient for the investigation of wake dissipation effects. For this study, a fine grid was defined to have 20 cells per rotor diameter, 128×128 AD cells (amount of cells in radial and azimuthal directions), ran at a residual limit of $1e - 05$. Whilst eight cells per rotor diameter was found sufficient, a justifiable

⁵ $\delta_v = 100 \cdot |v - v_f| / v_f$, where v is the calculated parameter, and v_f is the parameter's fine grid value for the particular case.

improvement in the converged results compared to a fine grid has been found when doubling this amount to 16 cells per rotor diameter. Thus, 16 cells per rotor diameter will be used for the simulations in this study.

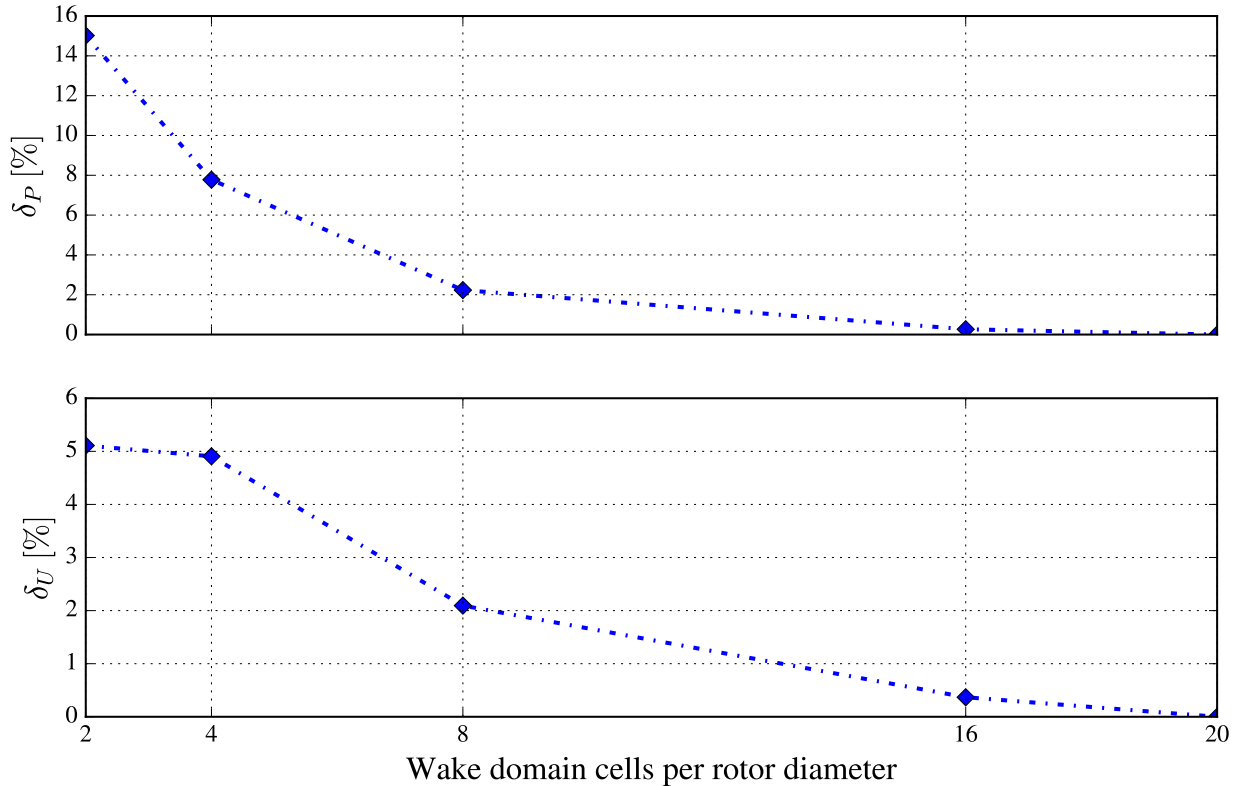


Figure 3.3: Wake domain grid spacing relative error for power and AD velocity deficit.

3.3.2 AD Grid

With the determined 16 cells per rotor diameter, an AD grid independence study was performed. The results in Figure 3.4 show that a 64×64 AD grid seems to perform almost as well as a 128×128 grid with four times less cells, hence a 64×64 AD grid will be used onward in the study.

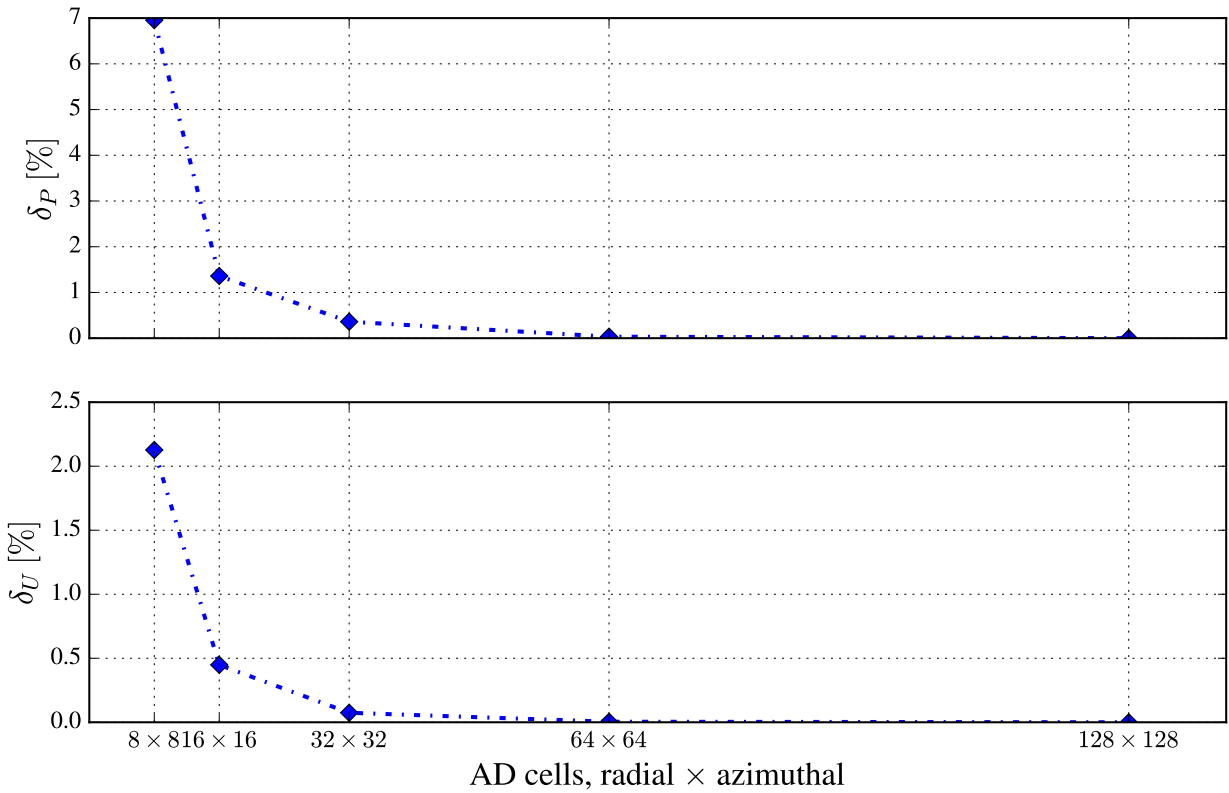


Figure 3.4: AD grid spacing relative error for power and AD velocity deficit.

3.3.3 Residuals Resolution

Finally, a resolution limit of the velocity component of the RANS CFD simulation should be chosen. In Figure 3.5 one may be deceived by the relatively small error in power when using a resolution limit of $1e - 02$, yet further analysis of the wind turbine wake shows a large discrepancy between this and the result of using a much finer resolution limit of $1e - 06$. A resolution limit of $1e - 04$ is found to be sufficient for this study, yet on recommendation and as per other investigations in PyWakeEllipSys, a conservative value of $1e - 05$ was chosen to be used.

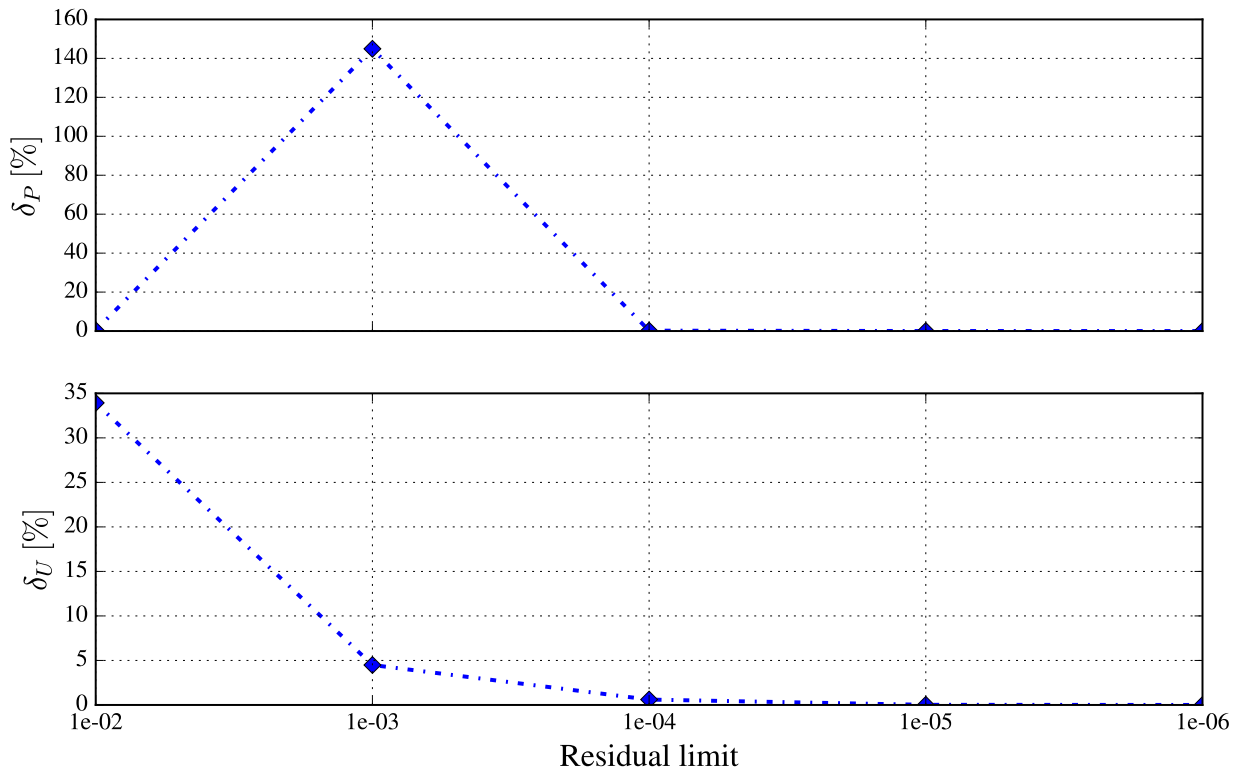


Figure 3.5: Residuals limit relative error for power and AD velocity deficit.

3.3.4 Numerical Grid Size

In order to ensure full development of the inflow boundary layer, along with avoiding the CFD tunnel blockage effect, the numerical grid is extended in all directions far from the wake domain, with a grid radius of 100 rotor diameters. In the vertical direction, the height of the first cell is 0.5 m, and this cell size increases exponentially, with the last cell being situated at $z/D = 25$. In the wake domain, the wind farm radius is extended by a margin of 3, 12 and 1.5 rotor diameters in the upstream, downstream and lateral directions respectively. The final numerical grid is visually represented in Figure 3.6, with the blue area showing the wake domain, the red dot representing the wind turbine, and with labelled boundary conditions. The coordinates $x = 0$, $y = 0$, $z = z_H$ in this thesis will be used to depict the wind turbine position, both in single wind turbine simulations and for the first wind turbine in row configurations (even though it is then shifted in the grid.)

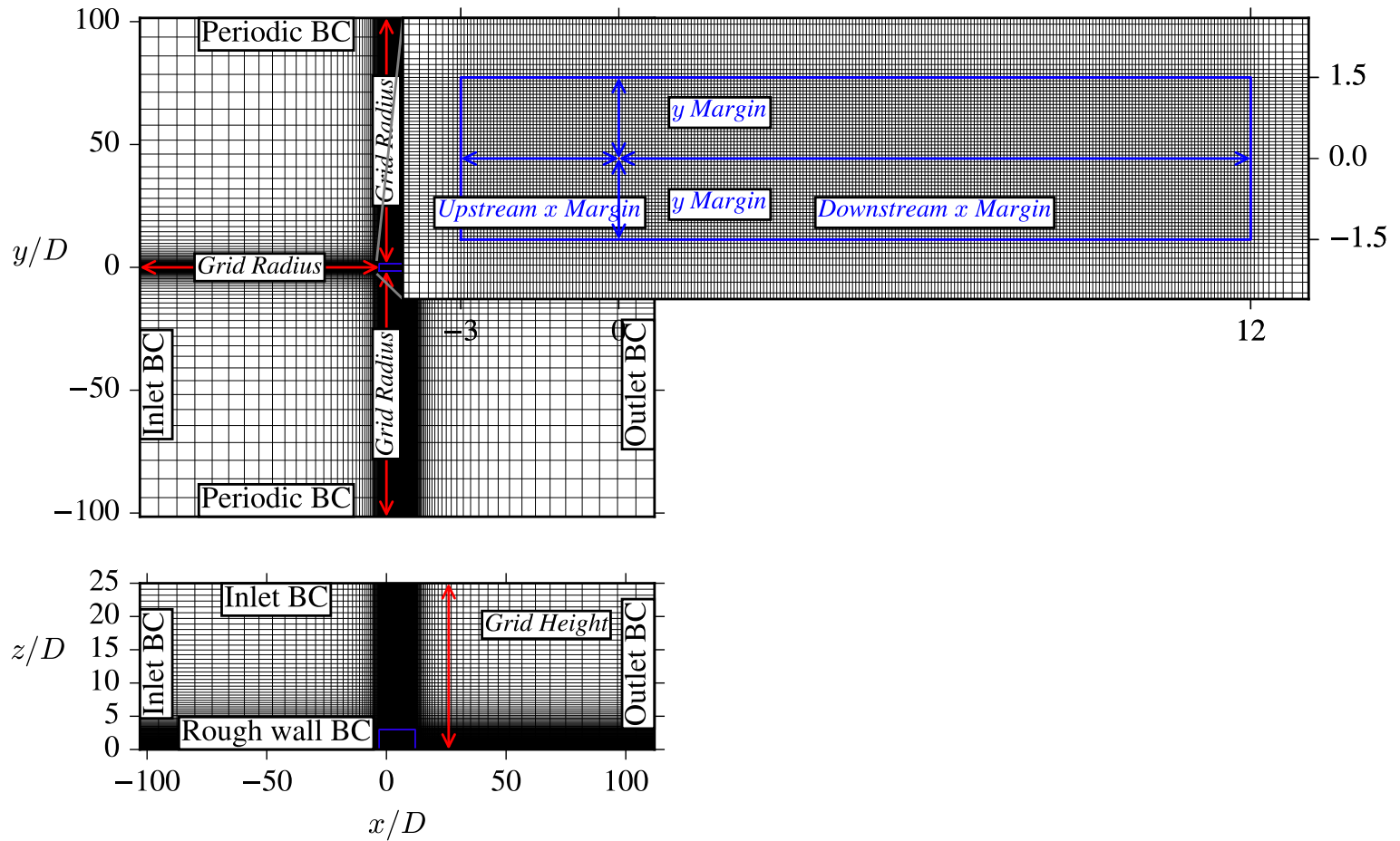


Figure 3.6: Numerical grid for a single wind turbine simulation. Top row: View of the grid from the top, with a zoomed in wake domain. Bottom row: View of the grid from the side.

To iterate, the grid study parameters arrived at by the grid independence study are collected in Table 3.1, with the other parameters kept at their default values (see PyWakeEllipSys documentation, closed source).

Table 3.1

Grid Parameter	Parameter Value
Cells per diameter (wake domain)	16
AD grid cells	64×64
Resolution limit	$1e - 05$

3.4 Other Parameters, Controlled Variables

PyWakeEllipSys has many model settings that can affect the results of a simulation. Parametric studies on these variables are outside of the scope of this thesis, as each may present

a research topic in and of itself. Thus, at the beginning of this study, the values of these parameters were tuned, to be kept constant throughout the study, as controlled variables. The values for these parameters, along with the reasons behind taking these, are given in this section.

3.4.1 Terrain, Inflow, Turbulence Intensity

Complex terrains are a possible input for PyWakeEllipSys, and are of interest for either onshore or certain (nearer to obstructions such as coasts, other wind farms etc.) offshore wind applications, both considered outside of the scope of this thesis. A flatbox grid, reminiscent of an offshore sea terrain, was chosen in order to best keep the focus on the blade design aerodynamics. This decision was further supported by the rising importance of offshore wind turbines in the industry at the moment [3].

In this flat terrain, all ambient turbulence is generated at the bottom rough wall which is defined by its roughness length [45]. Using the surface roughness length z_0 for an open sea of 0.2 mm [57], equation Equation 3.13 was used to arrive at an equivalent ambient turbulence intensity I_H at a hub height z_H of the examined wind turbine (119 m for the DTU 10 MW RWT).

$$I_H = \frac{\kappa \sqrt{\frac{2}{3}}}{C_\mu^{\frac{1}{4}} \ln \left(\frac{z_H + z_0}{z_0} \right)} \quad (3.13)$$

With the von Kármán constant $\kappa = 0.4$, and the turbulence model constant $C_\mu = 0.03$. The value of I_H of 5.9 %, calculated for the aforementioned conditions, was rounded to 6 % in the following investigation.

3.4.2 Wind Turbine Array Spacing, Layout, Wind Speed and Direction

In the upcoming wind turbine array studies, how close the wind turbines are to each other is an important parameter to be considered. As the wake velocity deficit is the highest right behind a wind turbine and slowly diffuses downstream, putting wind turbines too close together would significantly decrease the wind turbine row yield, fully exposing the wind turbine configuration to the effects of wake. However, putting the wind turbines too far apart would on the other hand not be desirable in real life scenarios, as wind farm developers want to increase their profits on their wind farms, and space is limited. Thus, the trade-off between the capital cost of investment into the number of wind turbines they can fit into their designated plot of land and the amount of energy produced, affected by the wakes, is born, and is currently considered by the research field of layout optimisation (see Subsection 2.3.1). Observing standard industry practices, along with wake research conventions, a wind turbine spacing of $x/D = 5$ is chosen for this investigation.

This is further complicated by the fact that as wind direction changes, and the wind farms vary in size and their geometry, wind farm layouts lead to the wakes interacting with the wind turbines in more complex ways. Thus, in the wind turbine array study in this investigation, only straight rows of three and ten wind turbines are considered. The row configuration is important from the perspective of showing extremes of the wake effect - as in real wind farms, wakes are rarely stacked straight on top of each other just like the wind turbines, thus a row configuration shows the highest possible loss of power due to the wake. This would thus allow us to find the highest possible gain in power thanks to the wake-diffusion rotor concept.

A single wind speed U_H of 8 m s^{-1} will be used. Furthermore, if wind direction is not directly towards the wind turbine but at an angle, due to this yaw effect, the wake is strongly affected. In order to sidestep the deep research field of wake steering (see Subsection 2.3.4, this investigation considers a single wind direction with direct inflow on the wind turbine (zero yaw angle).

3.4.3 Atmospheric Stability

The atmospheric boundary layer has a depth of about two kilometres, and a daily cycle of wind, temperature and humidity fluctuations can be observed, all of which affect the advection and the convection (horizontal and vertical movement) of the wind. Simplified and only looking at temperature variations, in a stable atmosphere (e.g. nighttime, cold surface), rising air parcels are pushed back by buoyant forces, thus suppressing turbulence. An unstable atmosphere (e.g. day, hot surface) would have the opposite effect, further displacing rising air parcels by buoyant forces, increasing turbulence [58].

As atmospheric stability is believed to influence power deficit in wind farm AEP calculations [51], a neutral stability layer will be assumed in the numerical investigation. This is modelled in the k - ε - f_P with a tuned model turbulence constant C_μ of 0.03, calibrated for neutral atmospheric surface layer flows.

Chapter 4

Results and Discussion

Three Joukowsky AD models of equivalent C_T but varying thrust distributions along the lengths of their blades are investigated, denoted $\bar{\delta} = 0.15$, $\bar{\delta} = 0.35$ and $\bar{\delta} = 0.60$. These represent a wind turbine with an inboard shifted thrust distribution, a baseline - conventional - wind turbine with a thrust distribution similar to that of the DTU 10 MW RWT, and a wind turbine with a thrust distribution shifted outboard, representing the wake-diffusion rotor concept, respectively. The simulations are run in a numerical grid representing offshore conditions, with a turbulence intensity of 6 %, and a freestream velocity $U_H = 8 \text{ ms}^{-1}$ at hub height. A normalised height coordinate $\tilde{z} = z - z_H$ is employed.

The focus of this study is how the wake-diffusion rotor concept, with its outboard thrust distribution, affects the wake produced by the wind turbine. This study also want to see possible benefits to using it compared to a baseline, standard wind turbine in terms of power capture thanks to its effect on the wake. The results of these simulations for a single wind turbine are presented in Section 4.1, after which the results for wind turbine rows of three and ten wind turbines are shown in Section 4.2. The chapter concludes with a discussion of relevant design considerations in Section 4.3.

4.1 Single Wind Turbine Study

A single wind turbine scenario is investigated first, in order to better understand the effects of varying thrust distributions under equivalent C_T on wake behaviour. The analysed parameters include velocity (deficit and profiles), turbulence intensity and momentum transport terms.

4.1.1 Velocity Deficit

Probing the wind turbine wake velocity on the rotor centre line could produce values which, due to the high locality and turbulence, do not represent the velocity deficit in the wake accurately. Thus, the measure $\langle U_{AD} \rangle / U_H$ of disk-averaged normalised velocity is used to quantify the velocity deficit⁶ in this investigation, in which $\langle U_{AD} \rangle$ is the averaged velocity over a fictitious, equivalent AD area to the wind turbine (just shifted upstream or downstream).

⁶A low value of $\langle U_{AD} \rangle / U_H$ indicates a high velocity deficit and vice versa.

Thus, this represents what overall velocity a fictitious wind turbine placed at the given location directly downstream of the wake would experience, which is strongly correlated to the power that the wind turbine could extract from the flow, making it a very popular measure in wake research due to its practicality.

The effects of increasing $\bar{\delta}$ and thus shifting the thrust distribution along the blade more outward is seen in Figure 4.1, clearly lowering the velocity deficit through an increased wake recovery rate. This effect is especially pronounced in the near-wake region, where the differences between the most inboard and the most outboard thrust distribution models ($\bar{\delta} = 0.15$ and $\bar{\delta} = 0.60$) is the largest. This region is nonetheless of little interest for the practical purposes of wind farms due to the large velocity deficit, which would severely decrease the production of wind farm arrays. This is due to there not being enough distance for the wake to mix with the surrounding flow and thus entrain ambient flow kinetic energy, replacing that which was extracted by the wind turbine.

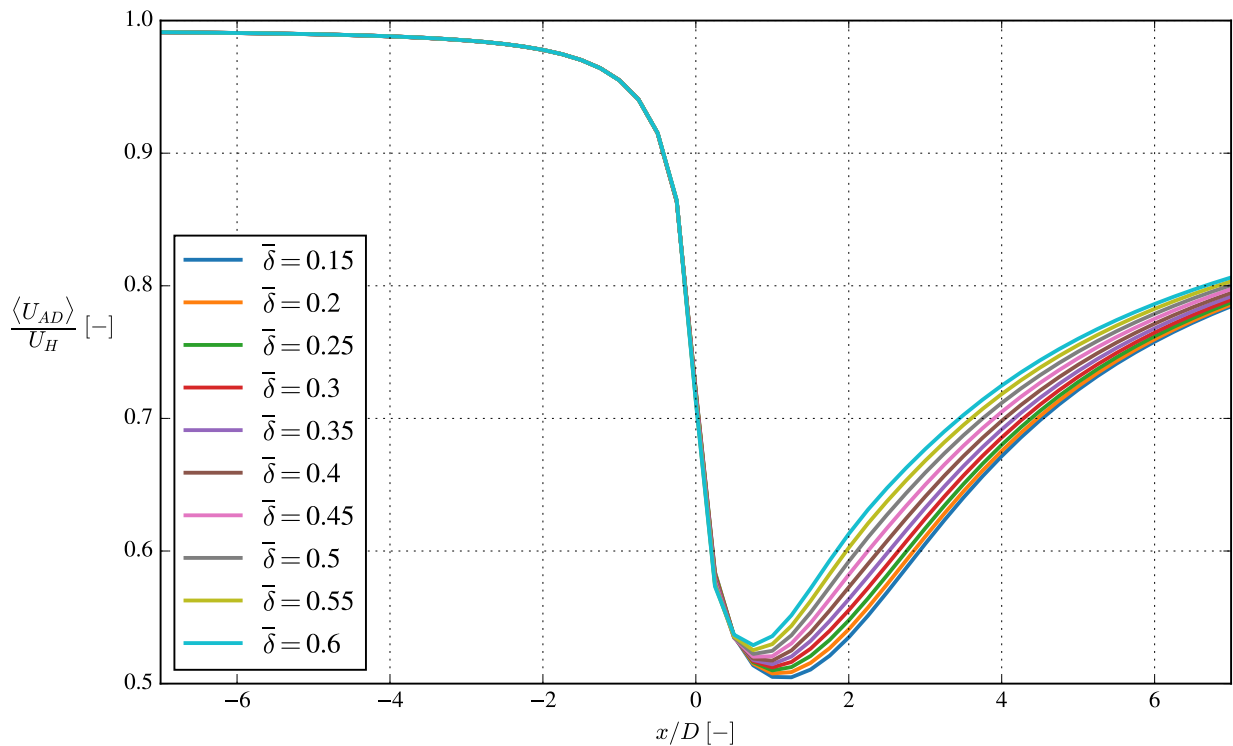


Figure 4.1: Streamwise velocity averaged over a fictitious AD area directly upstream and downstream of a wind turbine ($x/D = 0$) for varying $\bar{\delta}$.

At $x/D = 5$, a commonly probed distance downstream of the wind turbine in the field of wake research, the AD velocity deficits are equal to 0.72 and 0.76 for $\bar{\delta}$ of 0.15 and 0.60 respectively. As power in a flow is proportional to its velocity cubed ($P \propto U^3$), this leads to a theoretical range of roughly 18 % difference ⁷ in possible power capture for a second wind turbine, achieved just by manipulating the thrust distribution of the first upstream wind

$$^7 \frac{P_{\bar{\delta}=0.60}}{P_{\bar{\delta}=0.15}} \propto \left(\frac{(\langle U_{AD} \rangle / U_H)_{\bar{\delta}=0.60}}{(\langle U_{AD} \rangle / U_H)_{\bar{\delta}=0.15}} \right)^3 = \left(\frac{0.76}{0.72} \right)^3 = 1.176$$

turbine.

Further downstream (up to $x/D = 20$), the AD velocity deficits for the varying $\bar{\delta}$ converge. This is supported by the fact that - if a momentum balance point of view is taken - as the C_T is the same across all the $\bar{\delta}$ models, the same amount of momentum is extracted, which should lead to converged wake deficits in the very far wake. The opposite of this - a phenomenon where, a certain distance from the wind turbine, the AD velocity deficit of a lower $\bar{\delta}$ would be lower than that of a higher $\bar{\delta}$ - is seen in Kelley et al. [34] (which keeps the same C_T along the wind turbines, yet in which, the reader is reminded, the simulation has likely not statistically converged) and Zhang et al. [38] (in which the C_T is not kept the same), for the highlighted reasons.

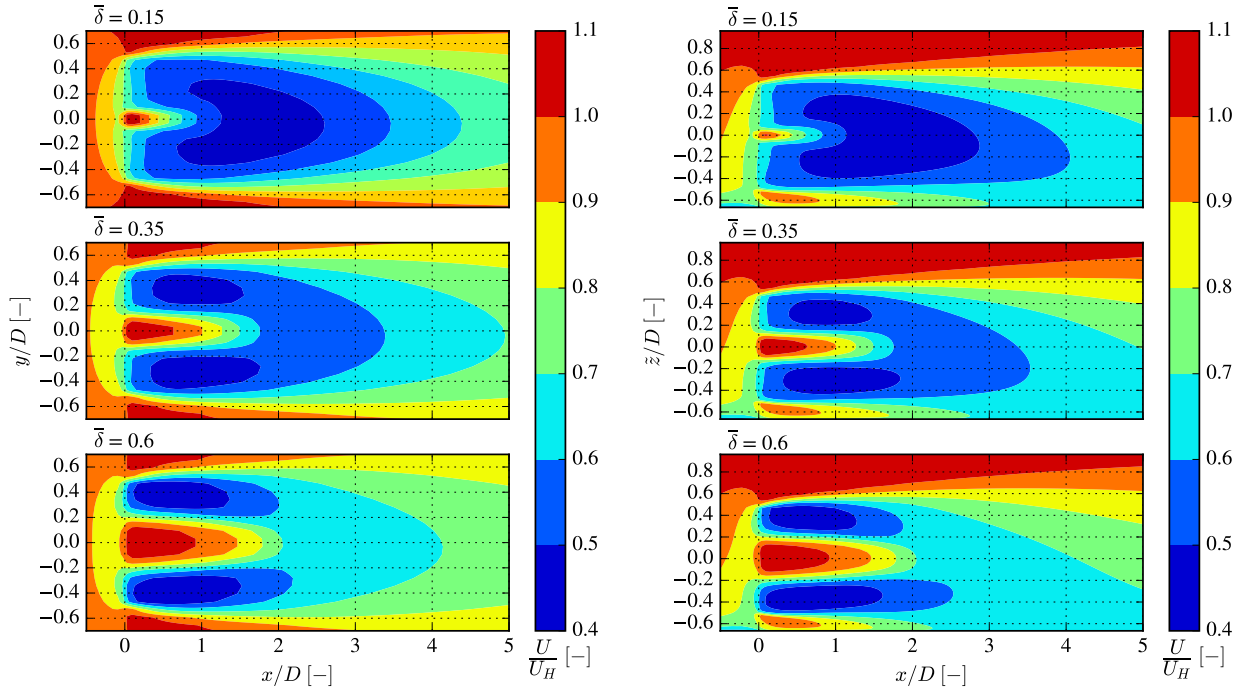


Figure 4.2: Velocity deficit contour plots for the Joukowsky AD model of varying $\bar{\delta}$ (at $x/D = 0$). Left column: view from the top. Right column: view from the side.

The contour plots in Figure 4.2 depict the large differences of the velocity deficit across the different $\bar{\delta}$ models, showing the clear superiority of higher $\bar{\delta}$ when it comes to wake-diffusion. There is a small area in the near wake, near the centre of the rotor in which the wind velocity remains high, surrounded on both sides by areas of very high velocity deficits closer to the rotor edges. This wake deficit profile of $\bar{\delta} = 0.60$ is highly similar to the wake encountered by Martínez-Tossas et al.[15] for high thrust, high RPM scenario wind turbine with a similar thrust distribution (for the Joukowsky AD model at this U_H , $C_T = 0.82$, compared to that of $C_T = 1.3$ of Martínez-Tossas et al.) This wake structure is also comparable to that of a multi-rotor wind turbine investigated by Baungaard [56] - in which the high thrust area near the edge of the rotor could be considered equivalent to the multi-rotors. This suggests a

similarity in their mechanisms of alleviating wakes.

The velocity deficits for $\bar{\delta} = 0.60$ are much higher near the rotor tip areas than for the other $\bar{\delta}$ cases, yet this higher velocity deficit dissipates much faster downstream of the near wake above $x/D = 2$, as also witnessed for a similar blade by Allen et al. [37]. It should be noted that, if integrated and averaged over a fictitious disk area, the velocity deficit of $\bar{\delta} = 0.60$ is still lower than that of lower $\bar{\delta}$ cases even in the very near wake as seen in Figure 4.1.

4.1.2 Velocity Profile

Velocity profiles across a vertical line at $y = 0$ for the varying $\bar{\delta}$ Joukowsky AD models at a set of distances upstream and downstream are shown in Figure 4.3. The first velocity profile at $x/D = -2.5$ (upstream of the wind turbine) shows the inflow boundary layer profile (see Subsection 3.4.1). At $x/D = 0$, that is, at the rotor, the most clear difference in the velocity deficit can be seen, with the wake-diffusion model $\bar{\delta} = 0.60$ experiencing the largest velocity deficits outboard on the rotor, closer to its edges. However, in the near wake at $x/D = 2.5$, it is already noticeable that the velocity deficit for this $\bar{\delta}$ also recovers the quickest, being smaller by up to almost 15 % at hub height compared to $\bar{\delta} = 0.15$. Further downstream in the far wake region, this difference quickly levels out.

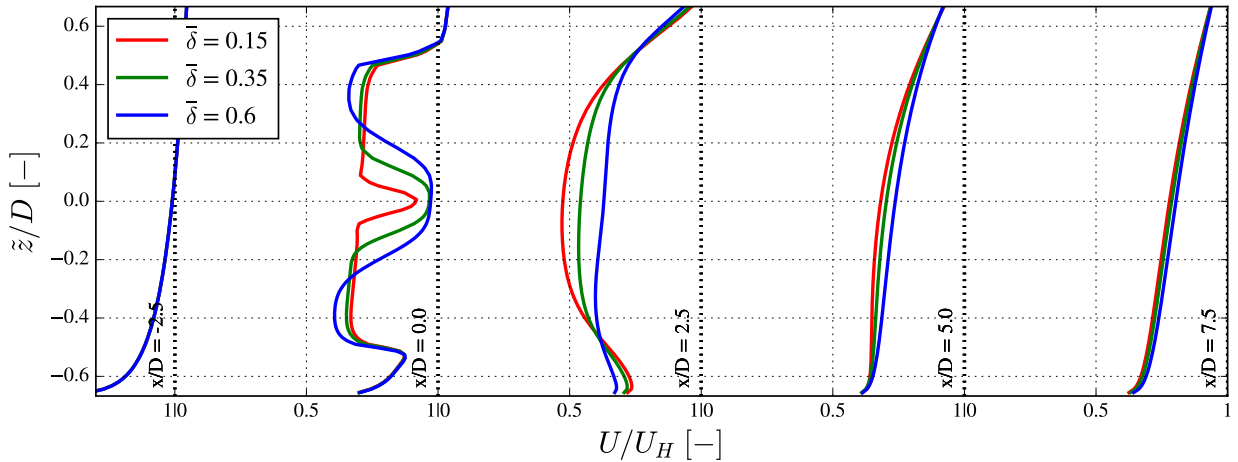


Figure 4.3: Streamwise velocity profiles along a line at $y = 0$ directly upstream and downstream of a wind turbine ($x/D = 0$) for the Joukowsky AD model of varying $\bar{\delta}$.

These findings about the wake-diffusion rotor's higher (local) velocity deficit in the near wake, yet lower ones in the actual area of interest where wind turbines in an array are placed, signifies the importance of studying wake behaviour beyond the near wake. This is once again another benefit of investigating the wake numerically as opposed to performing experimental aerodynamic studies, due to their inherent physical set-up limitations which often limit the possible investigated wake distance (see Section 2.2).

4.1.3 Turbulence Intensity

A way of conceptualising the mechanism of wake diffusion offered by the outboard-shifted thrust distribution is to consider it as a way of developing more turbulence (or ‘adding’ turbulence [11]) in the flow, resulting in increased mixing of the wake with the surrounding ambient flow and thus increasing kinetic energy entrainment into the wake.

Turbulent kinetic energy k (TKE) is a parameter that quantifies the kinetic energy associated with the eddies in the investigated flow. Figure 4.4⁸ shows more turbulence behind the near wake ($x/D > 2$) for the $\bar{\delta} = 0.60$ model than for those with more inboard distributed thrust forces. Right downstream of the rotor, the higher $\bar{\delta}$ model produces less turbulence near the root of the rotor (where there is less thrust), yet adds more turbulence near the rotor edges compared to the lower $\bar{\delta}$ models (as there is more thrust there).

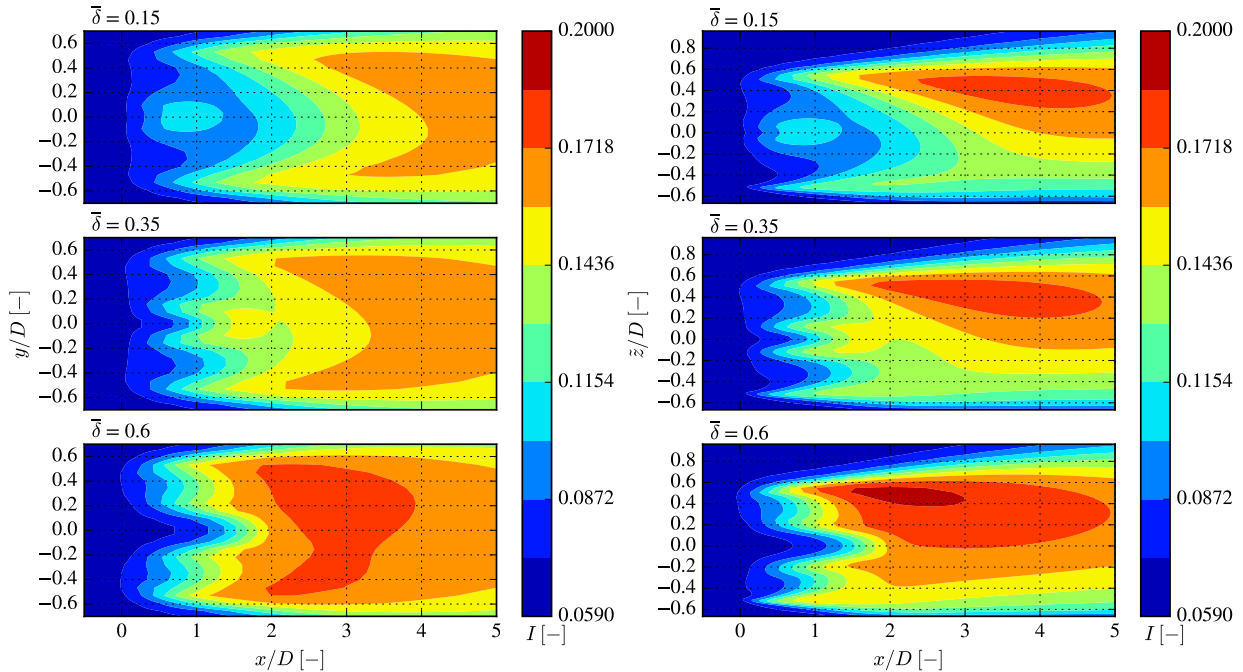


Figure 4.4: Turbulence intensity contour plots for the Joukowsky AD model of varying $\bar{\delta}$ (at $x/D = 0$). Left column: view from the top. Right column: view from the side.

The wake-diffusion concept configuration of $\bar{\delta} = 0.60$ which produces such a turbulence distribution in the wake thus seems to further promote the generation of higher turbulence further downstream, but still in an area where in a wind farm, a wind turbine would not be placed due to being too close to the first wind turbine. This should lead to more turbulent mixing downstream of the first wind turbine, explaining the lower probed velocity deficits in this area and further downstream. This result improves the outlook of using the wake-diffusion rotor concept in, for example, offshore wind farms, where the turbulent intensity is (most

⁸In this study, k is extracted and non-dimensionalised as by $\sqrt{\frac{2}{3} \cdot k}/U_H$, equivalent to turbulence intensity $I = \sqrt{\frac{1}{3} * \overline{u'_i u'_i}}/U_H$, often abbreviated as TI.

often) lower than in onshore ones, leading to longer-persisting wakes [59].

4.1.4 Reynolds Stresses and Stress Divergence

It is a common misconception to consider shear stresses the main cause of wake mixing in turbulence modeling - rather than the gradients of the shear stress. The lateral and vertical gradients of shear stress are the drivers of momentum transport throughout the wake as reminded to us by van der Laan et al. [60].

The gradients of streamwise Reynolds stresses⁹ (also called ‘stress divergence’) are shown in Figure 4.5, and the lateral and vertical ones are shown alongside each other in Figure 4.6. All the plots clearly show higher magnitudes of the shear stress gradients for higher $\bar{\delta}$ cases in the wind turbine’s wake, signifying more momentum transport across it.

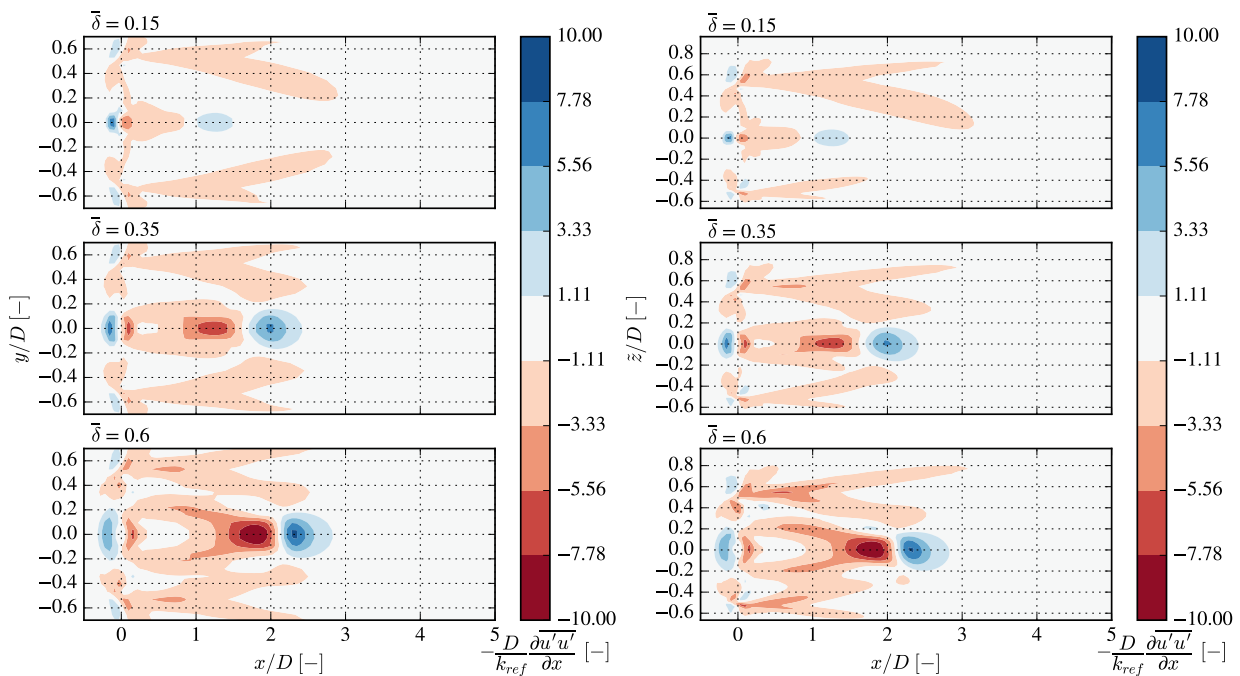


Figure 4.5: Streamwise momentum transport term contour plots for the AD Joukowski model of varying $\bar{\delta}$. Left column: view from the top. Right column: view from the side.

⁹Non-dimensionalised by $-D/k_{\text{ref}}$, where k_{ref} is the reference TKE at hub height upstream of the wind turbine.

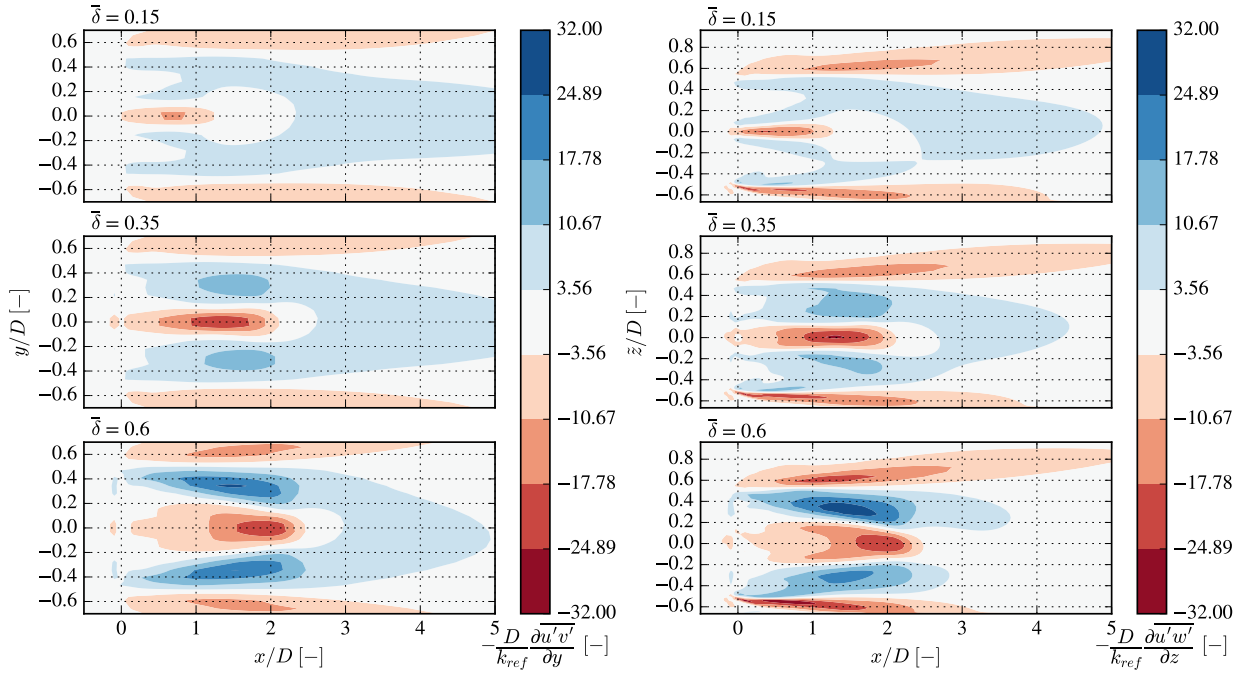


Figure 4.6: Momentum transport term contour plots for the AD Joukowsky model of varying $\bar{\delta}$. Left column: lateral stress gradients, view from the top. Right column: vertical stress gradients, view from the side.

To quantify the effect of the various $\bar{\delta}$ cases on the amount of momentum transport, the absolute values¹⁰ of the lateral and vertical momentum transports are integrated through Equations 4.1 and 4.2, and summed over the investigated wake areas.

$$M_{\text{lateral}} = \int_{y_-}^{y_+} \left| \frac{\partial \overline{u'v'}}{\partial y} \right| dy \quad (4.1)$$

$$M_{\text{vertical}} = \int_{z_-}^{z_+} \left| \frac{\partial \overline{u'w'}}{\partial z} \right| dz \quad (4.2)$$

This was performed along the wake domain $x = [-2D, 12D]$, using the limits of integration¹¹ $y_- = -2D$, $y_+ = 2D$, $z_- = 0$, $z_+ = 1.5D$. These were then normalised by the M_{lateral} and M_{vertical} obtained for the baseline $\bar{\delta} = 0.35$ case, to see the relative difference in momentum transfer across the wakes for the shifted thrust distribution cases.

This method of quantifying momentum transfer, inspired by the work of van der Laan [60], shows a clear trend of both more lateral and vertical momentum transfer in the wake, with a larger difference found for the vertical momentum transfer. These ranges indicate that roughly between 20 – 25% of the wake momentum transfer of the conventional design could be gained or lost by shifting the wind turbine’s thrust distribution. The increased momentum

¹⁰Done because the momentum loss in the freestream, part of which is included in the limits of integration, should be equal and opposite to the momentum gain in the wake.

¹¹The limits of integration have an almost negligible difference on the relative differences of the M values at these magnitudes.

transfer of the $\bar{\delta} = 0.60$ case support the higher wake-recovering effect hypothesised for the wake-diffusion rotor concept.

Table 4.1: Relative momentum transfer in the wake for the AD Joukowsky model of varying $\bar{\delta}$.

$\bar{\delta}$	$\frac{M_{\text{lateral}}{}_{\bar{\delta}=j}}{M_{\text{lateral}}{}_{\bar{\delta}=0.35}}$	$\frac{M_{\text{vertical}}{}_{\bar{\delta}=j}}{M_{\text{vertical}}{}_{\bar{\delta}=0.35}}$
0.15	0.89	0.86
0.35	-	-
0.60	1.08	1.10
ΔM Range [%]:	19	24

4.2 Row Study

In order to better quantify the potential benefits of the wake-diffusion concept for wind farms, analysis should extend from single wind turbine wake studies to studies on the wake's behaviour in a row configuration, along with a focus on energy yield. The same simulation parameters as in Section 4.1 are used, but now extended onto rows of three and ten identical wind turbines (denoted 3-WT and 10-WT rows respectively), spaced five rotor diameters apart (see Subsection 3.4.2).

4.2.1 Velocity Deficit

The velocity deficits shown in Figure 4.7 of the 3-WT row shows less development of a velocity deficit for the more outboard thrust distributions of the higher $\bar{\delta}$ models, which is even more pronounced in the 10-WT row depicted in Figure 4.8. For $\bar{\delta} = 0.60$, the largest lateral velocity deficit gradients are seen in the wake of the first wind turbine ($x/D = 0$), where there is a large difference in the velocity deficit behind the rotor centre and the rotor edges, just as described for the single wind turbine in Section 4.1. However, the consecutive wind turbines, experiencing lower inflow velocity, no longer have such pronounced velocity gradients in the wake along the rotor area, and the general distribution of the velocity deficit gradient is similar for all wind turbines after the second one, with only the magnitude of the velocity deficit gradually increasing.

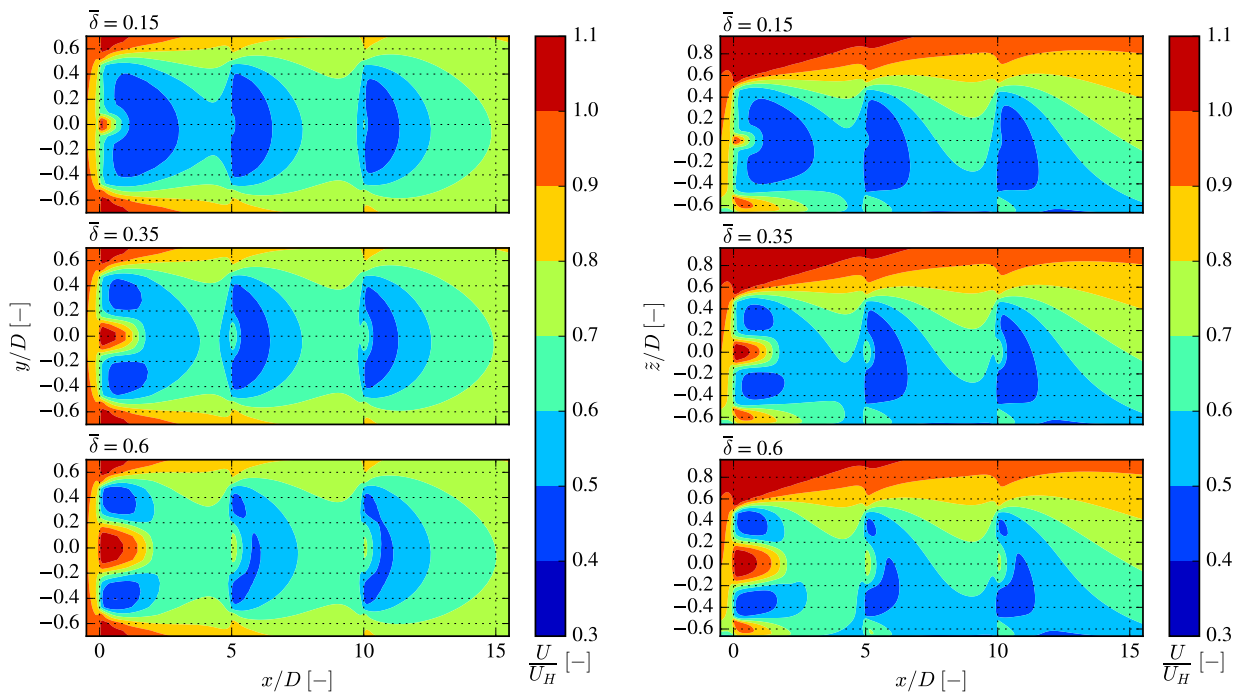


Figure 4.7: Velocity deficits for a 3-WT row for AD Joukowsky model of varying $\bar{\delta}$. Left column: view from the top. Right column: view from the side.

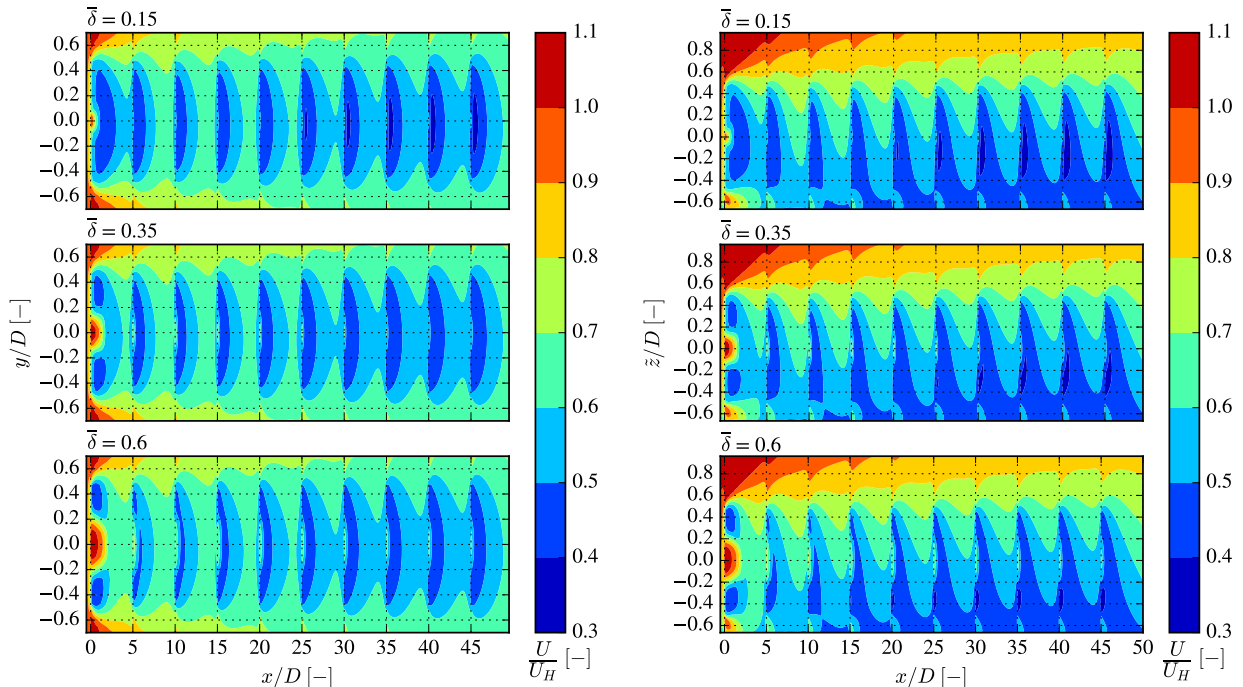


Figure 4.8: Velocity deficits for a 10-WT row for AD Joukowsky model of varying $\bar{\delta}$. Left column: view from the top. Right column: view from the side.

A closer top view is shown in Figure 4.9, in which the velocity deficit development down the 10-WT row is most visible across the varying $\bar{\delta}$ models. The general shape of the velocity

deficit field is more easily discernible, being largest between the first and second wind turbine, whilst being very similar for all wind turbines after the second one. This further suggests that the largest effect on the freestream flow in an array is exerted by the first wind turbine in the row, the cause and effect of which is further explored by the analysis of the other flow parameters. There seems to be insufficient energy entrainment by the wind turbine wake to replace the energy extracted by the wind turbines, leading to a progressively increasing wake deficit downstream.

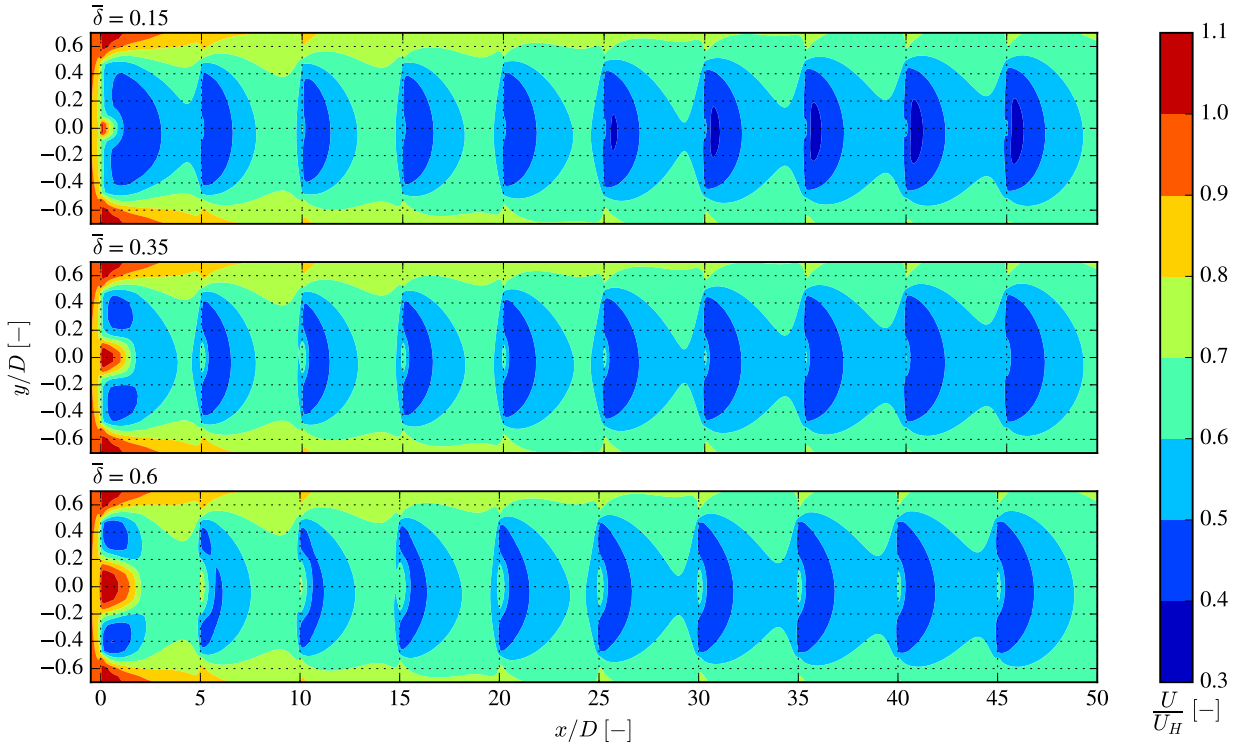


Figure 4.9: Velocity deficits for a 10-WT row for AD Joukowsky model of varying $\bar{\delta}$, view from the top.

4.2.2 Power Generation

In an ideal scenario, having a wind turbine rated at, for example, 10 MW, one would like a wind farm of N of these wind turbines to produce $N \cdot 10$ MW at their rated wind speed (the wind speed at which the wind turbine generates its rated power). However, in the worst case scenario such as featured in this study, with wind turbine wakes directly impacting on consecutive wind turbines in a straight row, the losses are large, as shown in Figure 4.10. Whilst the first wind turbine, unaffected by wakes, does produce energy (mostly)¹² proportional to the freestream wind speed, the same cannot be said for the others in the row.

¹²The first wind turbine does still experience wind farm blockage effects, a (small) reduction of upstream wind speed caused by energy extraction of the wind turbines. This effect can be most clearly seen in Figure 4.1, upstream of the wind turbine.

Each consecutive wind turbine in the row produces less and less power, dropping nearly to just 30 % of the first wind turbine's power by the tenth one for this worst case row scenario. That is 30 % of the power a wind farm developer would at first expect to gain by purchasing such a wind turbine for their project, when browsing the wind turbine manufacturer's catalogue. As the wake velocity deficit is not able to recover itself after each consecutive wind turbine, it gradually increases, allowing consecutive wind turbines in the row to extract less and less kinetic energy from the impinging flow, leading to less and less power capture.

A point of equilibrium, at which the wake deficit (and hence power generation) on the consecutive wind turbines would remain constant downstream, is nearly - but not yet - reached, as seen by the decreasing negative gradient near the last wind turbines in the row in Figure 4.10. This equilibrium would be reached more quickly (at an earlier wind turbine №) with increased wind turbine spacing.

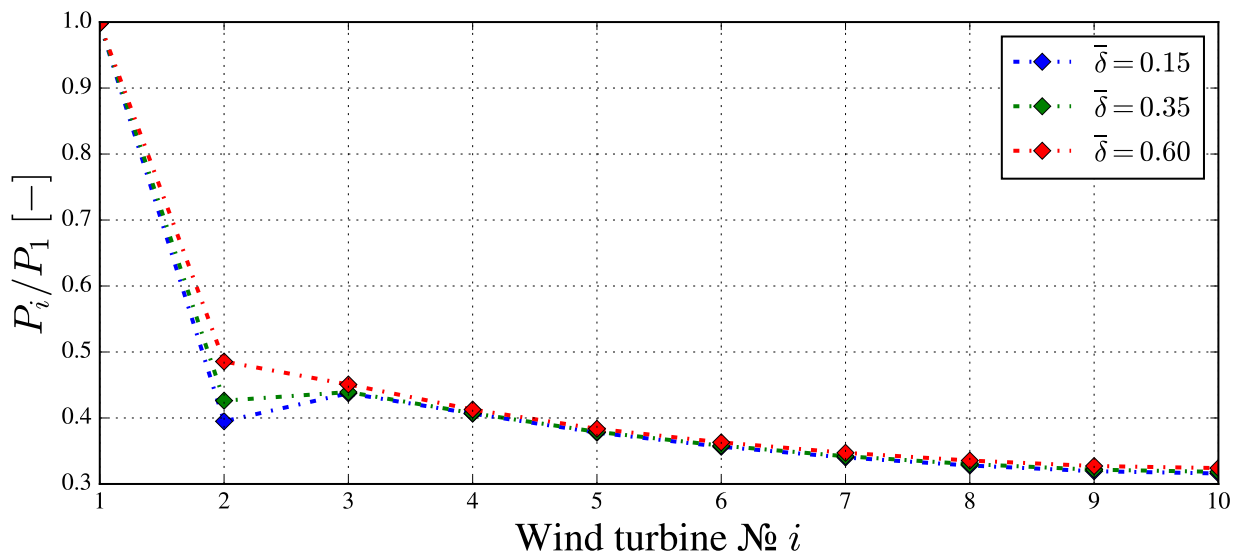


Figure 4.10: Power generation in a 10-WT row for the Joukowsky AD model of varying $\bar{\delta}$, normalised by P_1 .

As shown in the results in Table 4.2, the 3-WT and 10-WT rows generate just 62.5 % and 43.2 % (baseline design of $\bar{\delta} = 0.35$) of the ideal $N \cdot P_{U_H}$ MW scenario respectively, reiterating the possible impact of badly managed wakes on wind farm power capture and thus profitability. This worst case scenario wind directions highlights the relative importance of wind turbine spacing and layout optimisation for wind farm wake management.

Due to the effect of the lower velocity deficit experienced by the consecutive wind turbines in a row, it was assumed that using the wake-diffusion rotor concept ($\bar{\delta} = 0.60$) array would have increased power capture over one using the baseline design - an assumption which is confirmed by the results in Table 4.2. The power capture gains of using the wake-diffusion rotor in 3-WT and 10-WT rows of 3.8 % and 2.5 % respectively, suggest a diminishing effect along a wind turbine row of increasing size. The power capture losses incurred by using an inboard shifted thrust distribution rotor also diminish for the 3-WT and 10-WT rows, by

-1.8 % and -1.1 % respectively.

One immediate insight from these results is that the smaller the array size, the more beneficial a wake-diffusion rotor concept is for power capture, and the more disadvantageous it is to use a design with a more inboard shifted thrust distribution. The potential disadvantages of $\bar{\delta} = 0.15$ drop off slightly more with increasing array size (a relative difference of 41 % ΔP loss in power capture recovered by going from a 3-WT to a 10-WT row) than the advantages of $\bar{\delta} = 0.60$ (a relative difference of 34 % ΔP loss in power capture by going from a 3-WT to a 10-WT row).

Table 4.2: Wind turbine array power capture results. Left column: 3-WT row. Right column: 10-WT row.

3-WT row			10-WT row		
$\bar{\delta}$	P [MW]	ΔP [%]	$\bar{\delta}$	P [MW]	ΔP [%]
0.15	16.62	-1.77	0.15	38.56	-1.05
0.35	16.92	-	0.35	38.97	-
0.60	17.56	+3.79	0.60	39.94	+2.49
ΔP Range [%]:		5.56	ΔP Range [%]:		3.54

The power generation of the wind turbines with outboard and inboard shifted thrust compared to the baseline configuration are shown in Figure 4.11. Similar to the work of van der Laan and Abkar [61], for a multi-rotor configuration with a similar wake-diffusion effect, the largest increase in power is present in the second wind turbine of the row, and drops off with subsequent wind turbines. The magnitude of the ΔP_i range should be pointed out for how large it is - in using a wake-diffusion rotor concept, rather than one with an inboard shifted thrust distribution, the power capture of the second wind turbine can be increased by up to 21.3 % (from $0.926P_{\bar{\delta}=0.35}$ to $1.139P_{\bar{\delta}=0.35}$ for $\bar{\delta} = 0.15$ and $\bar{\delta} = 0.60$ respectively)¹³. This finding is in line with the insight from the analysis of the velocity deficits of Subsection 4.2.1, in that the wake-diffusion rotor concept has the largest impact on the wake of the first wind turbine, with diminishing returns for the other wind turbines down the row.

Furthermore, the gradients ΔP of Figure 4.11 are interesting to analyse, with their general shapes seemingly mirrored for the $\bar{\delta} = 0.60$ and $\bar{\delta} = 0.15$ models. The largest effect on power capture for either of the cases is present for the second wind turbine, diminishes for the third one, is the lowest at the fourth ($\bar{\delta} = 0.15$) or fifth one ($\bar{\delta} = 0.60$) which is a point of inflection, after which the effect of either power gain or loss starts slowly rising for the two cases as the row extends. Interestingly, for the $\bar{\delta} = 0.15$ case, there is almost no power loss compared to the baseline case around the fourth wind turbine.

¹³This is higher than the 18 % power gain range first derived from the different velocity deficits in Subsection 4.1.1, due to the nature of the C_P curve of the DTU 10 MW RWT used in this case. Wind turbines are designed to be most effective at kinetic energy extraction from the flow for certain ranges of wind speeds, depending on the design goals based on supposed site wind distributions.

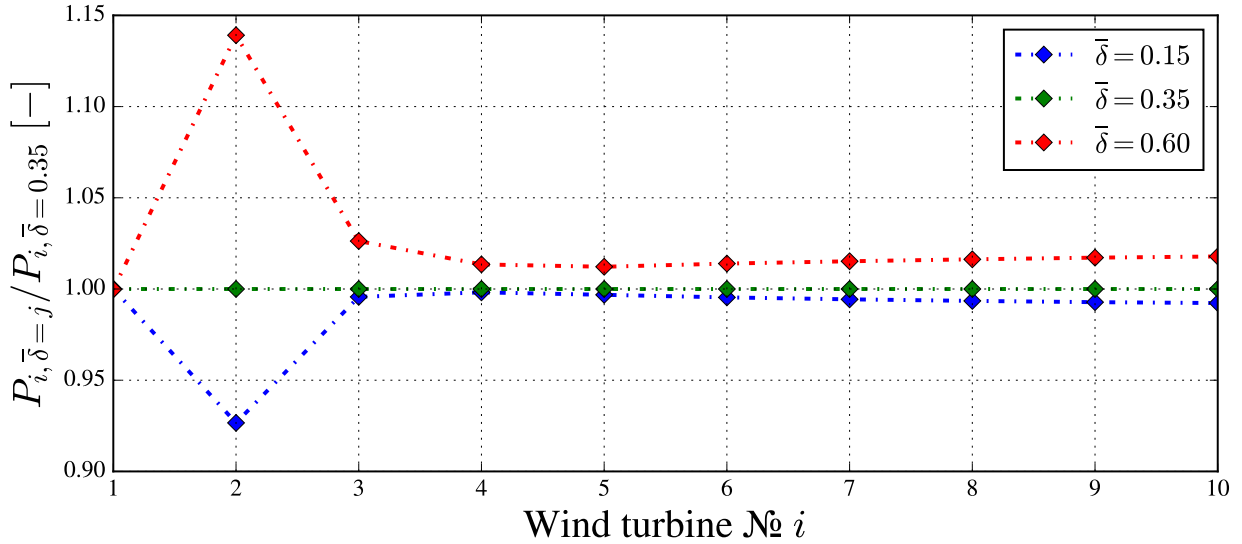


Figure 4.11: Power generation in a 10-WT row for the Joukowsky AD model of varying $\bar{\delta}$, normalised by $P_{i,\bar{\delta}=0.35}$.

There are multiple insights and possible recommendations stemming from these results. The ones pertaining to the $\bar{\delta} = 0.60$ case could argue for possible use of the wake-diffusion rotor concept either in larger wind turbine row arrays (due to its positive, increasing gradient seen in Figure 4.11), or for very short rows (due to the largest ΔP_i in the first wind turbines). In line with the concept of varying wind turbine types across a wind farm for maximum power capture introduced in Subsection 2.4.8 [36, 42], use of such a wind turbine on the edges of wind farms (where the wake-diffusion rotor would be the first wind turbine to experience unperturbed wind) can be recommended as well, depending on the specific site climate for maximum wake diffusion effect.

For the $\bar{\delta} = 0.15$ case, if the design were found to be superior to the wake-diffusion rotor for economic reasons (e.g. production costs due to structural considerations), then the use of them for the third-and-onwards wind turbine from the edge in medium-to-large wind farms could be argued for, as there is little change in power capture from the baseline (that is, if this effect persists in heterogenous wind turbine farm conditions).

4.2.3 Turbulence Intensity

In Figure 4.12 it can be seen that on encountering the first wind turbine, the flow experiences a large increase in turbulence intensity (from 0.06 up to 0.16, or almost a 170 % increase for the $\bar{\delta} = 0.60$ model). The second wind turbine, however, leads to a much lesser increase (from 0.16 to 0.21, or almost a 30 % increase for the $\bar{\delta} = 0.60$ model). As the wake turbulence dissipates further downstream of each rotor, the third wind turbine in the row adds in more turbulence such that the peak TI area after it is larger than in the wake of the second wind turbine, yet the maximum TI magnitude from the second wind turbine is not visibly increased,

leading to the lowest relative TI increase across the row.

This effect of adding turbulence is less pronounced for the models with thrust distribution shifted more inboard. Relative to the low initial turbulence intensity of the undisturbed flow (simulating offshore wind farm conditions), the effect of the first wind turbine on the present turbulence is the most substantial. It is this first highest addition of turbulence into the flow that has the most profound wake-diffusing effect, which explains the largest relative gains in power capture of the second wind turbine and wake recovery as seen in Subsections 4.2.2 and 4.2.1 respectively, and is a conclusion shared by van der Laan and Akbar [61] in their work with the multi-rotor wake turbine. Thus, the consecutive wind turbines in Figure 4.11 show much smaller differences in power capture, as no matter the $\bar{\delta}$ model used, the TI gain from which the outboard thrust distribution benefits the most (thanks to the increased mixing effect on kinetic energy entrainment) at the first wind turbine diminishes down the array, as the same absolute magnitude of TI is reached for the arrays.

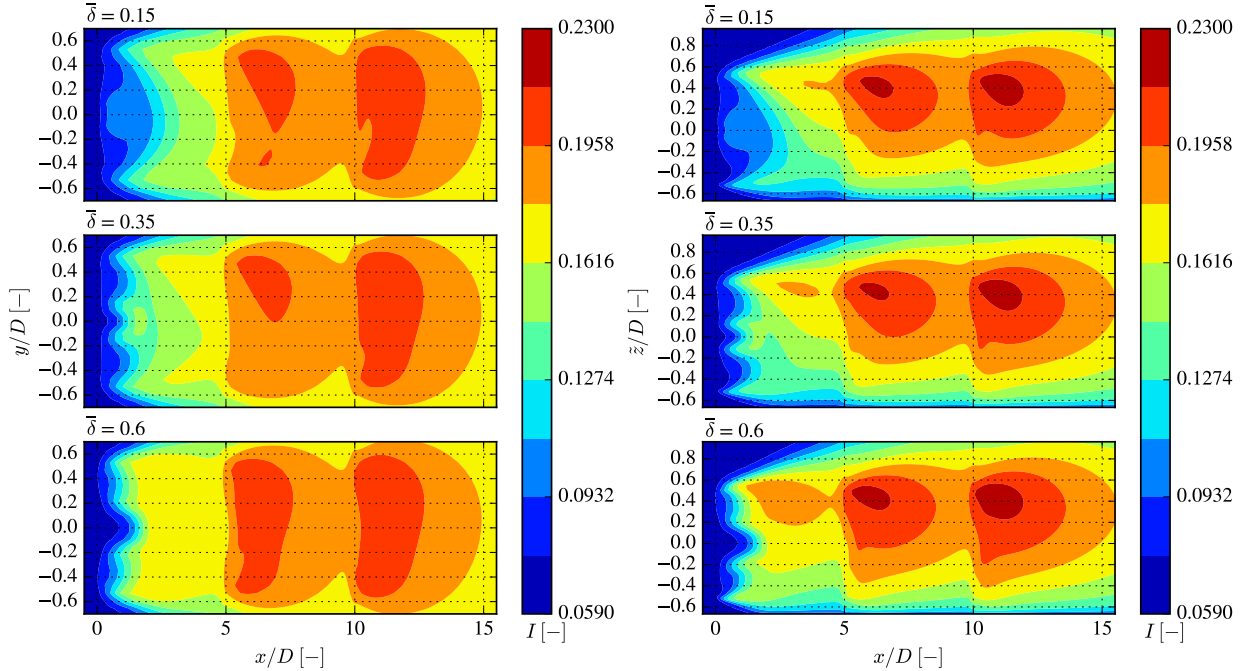


Figure 4.12: Turbulence intensity for a 3-WT row for AD Joukowsky model of varying $\bar{\delta}$. Left column: view from the top. Right column: view from the side.

Figure 4.13 especially shows how a peak TI (highest magnitude along the highest area) seems to be achieved by the third wind turbine, after which the TI (now both peak magnitude and area size) starts dropping off downstream throughout the wind turbine row. This peak TI is encountered at the third wind turbine for all three investigated values of $\bar{\delta}$. This explains the diminishing effectiveness of the wake diffusion concept in wind turbine arrays of increasing size, if one were to take the wake-diffusion rotor concept as a turbulence contributor such as described in Subsection 4.1.3.

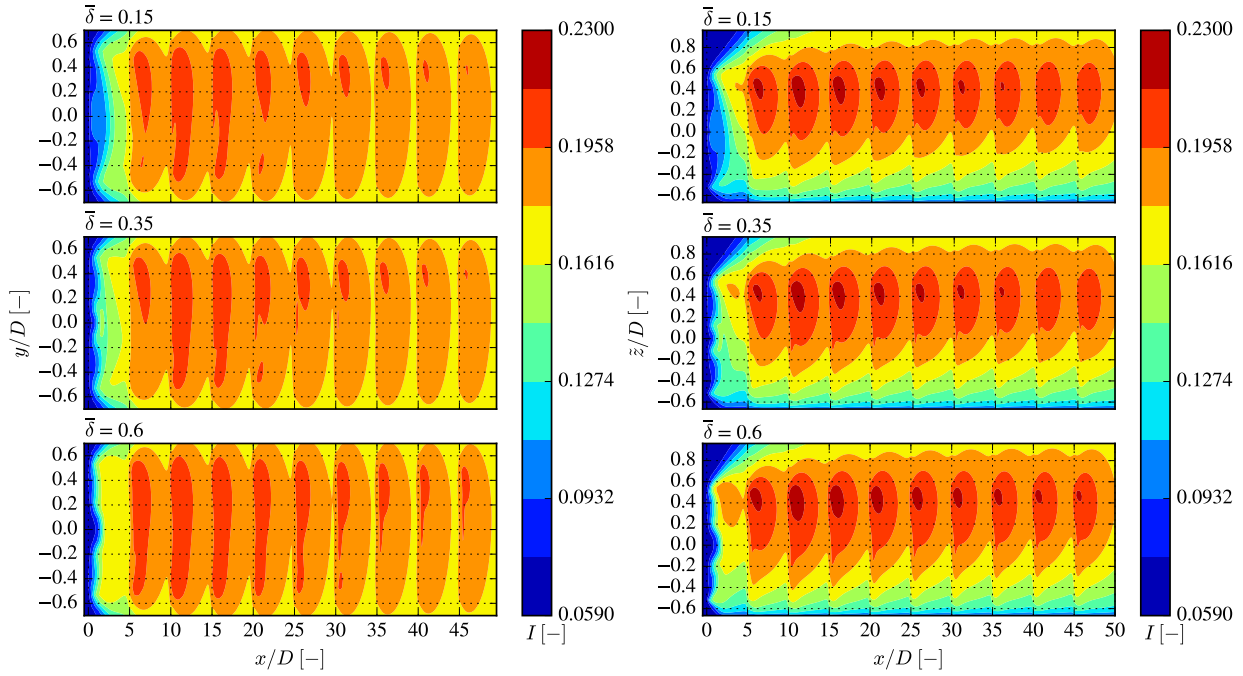


Figure 4.13: Turbulence intensity for a 10-WT row for AD Joukowsky model of varying $\bar{\delta}$. Left column: view from the top. Right column: view from the side.

The increased turbulence in the wake, provided by the wake-diffusion rotor, whilst beneficial for power generation, could lead to increased fatigue loads, not treated in this study [5]. Not only does this have structural implications for the wind turbine design, but a tradeoff on the economic costs and benefits of this effect is called for, as these turbulence-induced fatigue loads are considered one of the main factors which determines wind turbine lifetime [10].

With this evidence behind the physical mechanisms of the concept, the conclusive recommendations of Subsection 4.2.2 are confirmed. The wake-diffusion rotor concept, for maximum effectivity, should be either used for either the very small or the very large wind farms, or possibly on the wind farm's edges (as the first wind turbine).

4.3 Design Considerations

The Joukowsky AD rotor, taking C_T and C_P curves of the wind turbine as input, likely differs in these compared to how a physical implementation of this concept would perform. In Knauer [6], a small overall loss in power capture for a wake-diffusion rotor concept is expected, as there is a focus on decreasing energy extraction near the root of the rotor, without compensating for the loss in C_T by increasing the thrust force and power generation in the outer part of the rotor. The expectation is that a small power loss in individual wind turbines using the wake-diffusion rotor concept would be offset by the larger power capture in consecutive wind turbines in a wind farm configuration. A question thus arises - what is the maximum amount of individual wind turbine power loss which would still be possible to be offset by the wake-diffusion effect?

As with many such questions, the answer seems to be “it depends”. This thesis has clearly identified several insights and trends pertaining to the wake-diffusion rotor design, which can certainly come in handy for potential researchers meaning to realise this concept further. Furthermore, this study features the investigation of a worst-case scenario, that is of a wind turbine row with directly impinging wind turbine wakes, which in a realistic wind farm scenario, may occur for only a fraction of a year. This raises the question of the magnitude of the possible benefits of using a wake-diffusion rotor on AEP - that is, taking into account the wind farm layout, along with varying wind speeds and directions over a year. Knowing the results of this study, it seems certainly possible that for certain combinations of wind farm layouts and wind climates, using wake-diffusion rotors could increase AEP. However, if the wake-diffusion rotor design implied individual wind turbine power loss, then depending on the magnitude of that loss the design could surely become disadvantageous for certain scenarios.

Chapter 5

Conclusion

This thesis aimed to explore the potential benefits of the wake-diffusion rotor concept, which can be described as a wind turbine design with a thrust distribution that is shifted outboard on the rotor, closer to the edges of the blades. A literature study is conducted, and based on a quantitative and qualitative analysis of numerical simulations, several conclusions are made on this concept.

An analytical actuator disk model in a RANS CFD flow solver (PyWakeEllipSys) is used, which can model wind turbines with differently distributed thrust across the wind turbine blade whilst keeping the overall C_T the same. A single wind turbine simulation is performed to study the wake behaviour of three thrust distributions - a conventional design, a design with inboard shifted thrust distribution, and an outboard shifted thrust distribution, representing the wake-diffusion rotor concept. Shifting the thrust distribution across the blade more outboard leads to a reduction of the wake velocity deficit downstream of the rotor. This effect on the velocity deficit is strongest around the near wake region ($x/D = 2$) and slowly dissipates further downstream, with the velocity deficits converging for all types of investigated thrust distributions in the very far wake. The wake-diffusion rotor concept also produces more turbulence and momentum transfer in the wake.

In row studies of three and ten wind turbines, the largest differences in the wake behaviour are found downstream of the first wind turbine. The wake-diffusion rotor concept row is compared to the baseline case. Total power generation was found to be higher (3.8 and 2.5 % for the 3-WT and 10-WT rows, respectively), with the highest relative gains in power capture found in the second wind turbine in the row (13.9 %). This power gain from using a wake-diffusion rotor concept is also present, although in a smaller magnitude, in consecutive wind turbines down the row. An analysis of turbulent kinetic energy in the row's wake found the wake-diffusion rotor concept adding the most turbulence into the flow with the first wind turbine. Peak levels of turbulence are reached around the third wind turbine for each thrust distribution model, and then slowly decrease down the row. The largest gain in turbulence in the wake of the first wind turbine is proposed to be the reason behind the largest power gain observed in the second wind turbine in the row, and the attainment of peak turbulence and its consecutive drop-off is considered to explain the diminishing benefits of using the wake-diffusion rotor concept down the row. Given the fidelity of RANS model used in this investigation, it can be concluded single digit percentage increases in power generation could

be expected for certain scenarios.

The inboard shifted thrust distribution shows the opposite effects of the wake-diffusion rotor concept, leading to larger velocity deficits, less added turbulence, less momentum transfer and lower power capture (-1.8 and -1.1% for 3-WT and 10-WT rows respectively, compared to baseline case) in a row configuration - with the highest relative losses in power capture in the second wind turbine (-7.9%). The absolute magnitudes of the disadvantages caused by an inboard shifted trust distribution are lower than the possible benefits gained by an outboard shifted one (with the baseline case defined as in this study).

The outboard shifted thrust distribution of the wake-diffusion rotor concept, causing large shear stress gradients due to large thrust near the rotor edge and small thrust near the root, leads to more momentum transfer in the wake and thus turbulent mixing. This is considered to be responsible for faster breakdown of helical vortex tip structures, subsequent increased kinetic energy entrainment of the wake and thus the wake diffusion effect.

Multiple ways of changing the wind turbine blade forces, ranging from blade geometry design to using flow devices on the blade and individual wind turbine control schemes are highlighted in the literature study. These are considered for their potential use in achieving the wake-diffusion rotor concept thrust distribution. On top of these, an overview of wind-farm level wake mitigation methods is also given, the combination of which with the wake-diffusion rotor concept could likely lead to even larger power capture gains across wind farms.

From the results of this study, recommendation can be made in using the wake-diffusion rotor in either very small or large wind farms. Using the wake-diffusion rotor wind turbines on the edges of wind farms to maximise the power capture gains of the second wind turbine in the free stream flow is also a possibility. Wind farms with layouts and wind climates that lead to strong and frequent wake interactions between the turbines, similar to the row scenario investigated in this study, are likely to gain more benefits compared to other scenarios. The benefits should also prove to be the highest for sites with low ambient turbulence intensity, such as offshore wind farms, and lower for sites with higher turbulence intensity, such as onshore ones.

Future Work

The shifting of the thrust distribution outboard through changes to blade geometry, flow devices or individual wind turbine control schemes bring along aeroservoelastic concerns that were not addressed in this study, which focused on the aerodynamics of the wake. Optimal ways of achieving this thrust distribution could be investigated.

The various ways of wind-farm level control schemes and other wake alleviating methods could be investigated in combination with the wake-diffusion rotor concept in order to arrive at a combined, multi-level approach at alleviating the negative effects of wakes on wind farms. This analysis could extend from simple power generation to load alleviation and ancillary

grid services.

The importance of modeling the thrust distribution in order to better predict the wake behaviour is confirmed by the study, and could be considered valuable information for both developers and users of engineering wake models. Existing engineering wake models could have their parameters tuned in order to account for varying thrust distributions, which provides a possible future avenue of research.

Whilst the benefits of the wake-diffusion rotor concept have been confirmed, if such a design would come at a cost in individual wind turbine power generation, the concept would become highly dependent on the particular wind farm layout and wind climate. First, the acceptable level of individual wind turbine power generation that would still bring benefits in wind farms could be investigated. Furthermore, investigation could be done on wind turbine spacing, wind farm layout, turbulence intensity, atmospheric stability, and wind climate (considering different combinations of wind speeds and directions) and their effects on the power capture in wind farms using the wake-diffusion rotor concept. Using higher fidelity turbulence models than RANS (e.g. LES) could be considered, to better increase the accuracy of the possible effects. With these insights, and a more realised wake-diffusion rotor design, full wind farm AEP simulations should be performed to quantify the possible AEP gains.

The turbulence-adding effect of the wake-diffusion rotor concept shows promise in being beneficial for power capture if used at the edges of the wind farms, and the quantification of these benefits associated with its use in nonhomogeneous wind turbine type wind farms could be investigated to greater depth. The higher turbulence may come at the cost of higher fatigue loads on consecutive wind turbines in its wake, which would benefit from research that would help in trading off the aerodynamic gains against the lower wind turbine lifetime associated with fatigue loading.

Appendix A

Wake-diffusion Rotor Design

Although not considered in the original scope of the study due to how large of an undertaking a more feasible and complete wake-diffusion rotor design would be, some exploration of the concept's design was conducted nonetheless. The numerical tools and models used for this design exploration are explained in Section A.1. The design process is described in Section A.2, and the results and discussion of this redesigned wind turbine's wake are given in Section A.3.

A.1 HAWC2S, PyWakeEllipSys Airfoil AD Model

HAWCStab2 is a frequency based aeroservoelastic code for steady states computation, most often used for stability analysis of wind turbines. HAWC2S is a command line version of this code, and was chosen to be used in this investigation as a part of a design tool for the wake-diffusion rotor, as a more verified and validated alternative to writing a new blade element momentum (BEM) code for the study.

Simply speaking, compared to PyWakeEllipSys, HAWC2S could be considered to be a higher fidelity code when it comes to single wind turbine performance, yet PyWakeEllipSys is superior for investigating the wake due to the RANS CFD code present within. The quick rotor performance evaluation allowed by HAWC2S was necessary for iterative design purposes (i.e. simulation runtime of seconds compared to tens of minutes).

As the airfoil AD forcing method in PyWakeEllipSys (described in the following Section A.1) does not model aeroelastic effects and assumes rigid blades, it is chosen not to include aeroelastic effects in the HAWC2S analysis of the wind turbine. The simple HAWC2S model further uses a normal BEM dynamic induction method and a Prandtl tip loss model. No dynamic stall model is used, as this phenomenon is not present for the investigation in question.

A Python design tool is written and used for the purposes of this investigation, which incorporates HAWC2S. This tool takes the HAWC2S DTU 10 MW RWT blade geometry input file (along with others), allows the user to change the blade geometry, evaluates the

new wind turbine's performance using HAWC2S, and outputs blade geometry files for the new design that can be used in subsequent PyWakeEllipSys simulations, to investigate wake behaviour.

PyWakeEllipSys Airfoil AD Model

PyWakeEllipSys has a blade-geometry based AD forcing method working on similar principles to blade element momentum (BEM) codes, such as the one found in Hansen [7]. The input files required by this model include airfoil descriptions (lift, drag and momentum coefficients tables at various angles of attack) along with a blade geometry description (chord length, blade twist angle and relative thickness distributions). This AD model is used for both the DTU 10 MW RWT and the redesign for simulation of the wake behaviour in PyWakeEllipSys.

A.2 WDR 10 MW Design

The DTU 10 MW RWT wind turbine was redesigned in this investigation, the process of which provided useful insights on the wake-diffusion rotor concept. This redesign will be referred to as the WDR 10MW onward, its name inspired by its predecessor. It should be emphasised that a feasible design for a wake-diffusion rotor was not the goal nor a desired deliverable of this investigation, due to the size of the undertaking, and is considered outside of this project's scope. Aerodynamic and production aspects of the design are not taken into account, due to a pure focus on the aerodynamics of the wake. The design space was confined to the blade's chord and twist, with the airfoil distribution of the DTU 10 MW RWT untouched.

The shaft tilt and the precone angles (5° and 2.5° respectively) were removed from the DTU 10 MW RWT for the purposes of the redesign, as PyWakeEllipSys can not take these as an input.

Over thirty designs were produced, with subsequent analysis of their wake velocity deficits at $x/D = 5$. The insights on the most effective wake-diffusion producing blade alterations coincided with input from Knauer [6], based on personal correspondence. The design strategy that was found to lead to the highest increase in the wake-diffusion effect, at the lowest cost of the individual wind turbine power loss, was to decrease the energy extraction from the flow by the rotor root area as much as possible. This was attained through finding an angle of attack α that minimise both the coefficients of lift and drag (C_L , C_D) of the airfoils near the root (found to be $\alpha = -2^\circ$).

The length of the blade up to which the ‘ventilating’ portion with low thrust is to extend was found to be an important design parameter by this investigation. The wake-diffusion rotor’s patent gives ranges for the radially-inner, ventilating portion of the blade of between $15 - 40\%$, more preferably $20 - 30\%$ and most preferably between $20 - 25\%$ of the blade [6]. There is expected loss of individual wind turbine power associated with making the radially-inner area near the root of the rotor suboptimal in power capture, letting a jet of high-energy air through into the wake. This individual wind turbine power loss is however justified by the potential gain in downstream wind turbine energy generation,

expecting a lower wake deficit, and thus more kinetic energy in the wind which it could extract.

To better determine the exact length of the blade to be made a ventilating portion - in which the energy extraction was to be minimised - the power contribution along the blade of a DTU 10 MW RWT was analysed, as depicted in Figure A.1, for a similar simulation scenario of Section 4.1. The results of Figure A.1 are also presented in Table A.1, and help see why values above 40 % are not considered by Knauer due to the high possible power losses. The first 25 % and 40 % of the blade makes up for 6 and 20 % of the rotor's area respectively. The 20–25 % range seem to be considered the ideal part for the ventilating portion of the blade, as the potential power losses are still quite low, and almost double in magnitude were one to extend further.

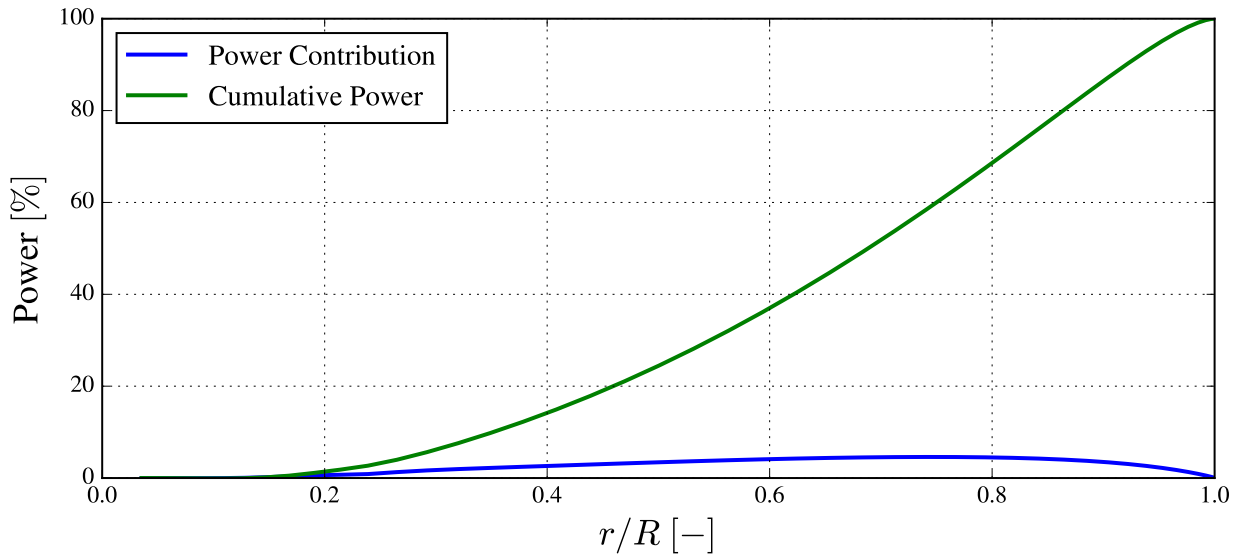


Figure A.1: DTU 10 MW RWT power generation contributions along the rotor.

Table A.1: Cumulative power contributions of the DTU 10 MW RWT rotor up to given r/R .

$r/R [-]$	Cumulative Power [%]
0.15	0.2
0.20	1.4
0.25	3.2
0.30	6.2
0.35	9.9
0.40	14.2
0.50	24.4

This minimum energy extraction angle of attack at the root of the blade was achieved through an iterative design process of twisting the blade, and the chord length at the root of the blade was also decreased (by up to 1 m). The resulting chord and twist distributions, compared to the DTU 10 MW RWT, are presented in Figure A.2. The force distributions along the WDR

10 MW blade shown in Figure A.3 depict the large intended decrease in thrust force on the root of the blade. The large twist of the WDR 10 MW comes from the angles of attack experienced by the DTU 10 MW RWT at the root of up to 60° , where the blade is very cylindrical.

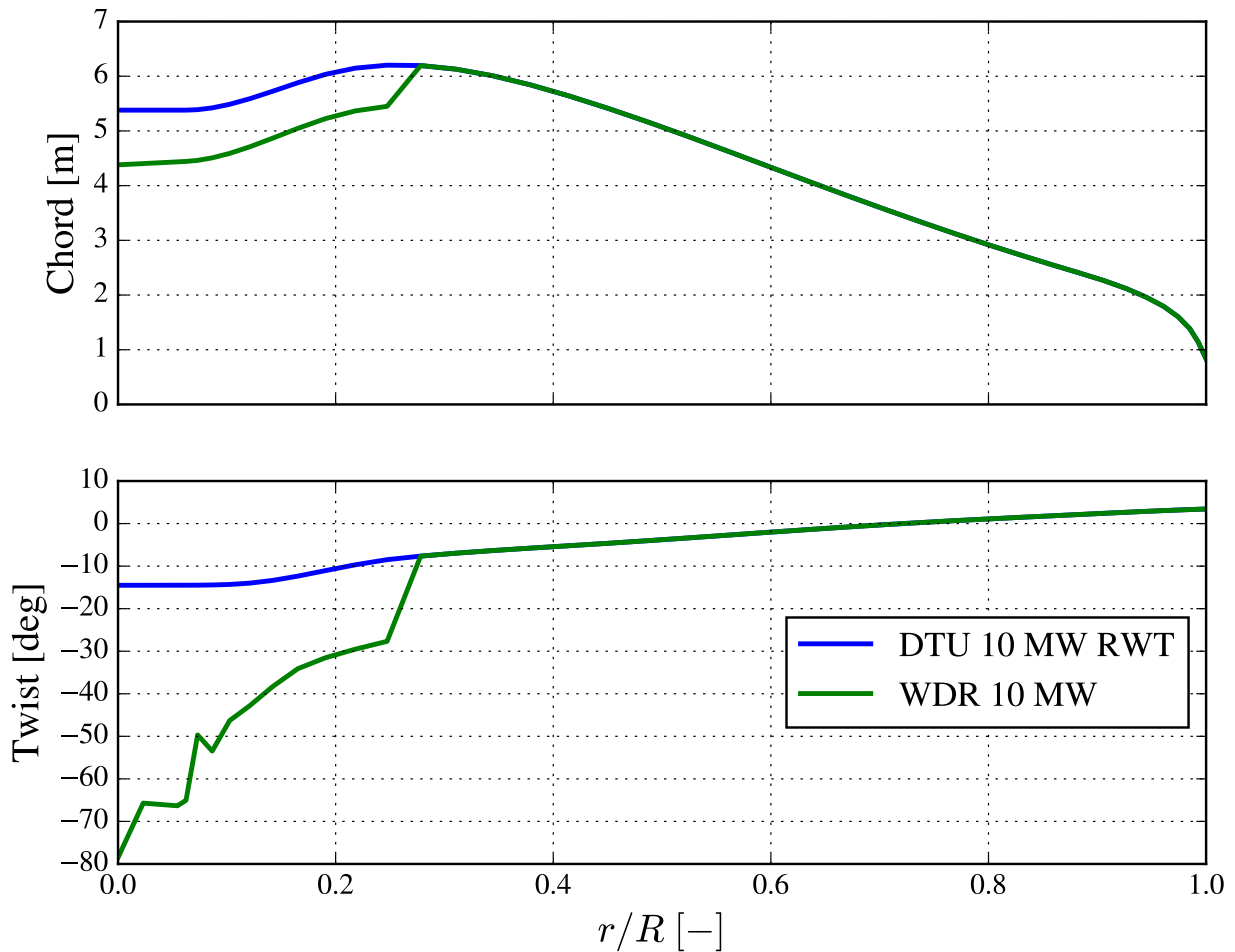


Figure A.2: WDR 10 MW chord and twist distributions along the blade length.

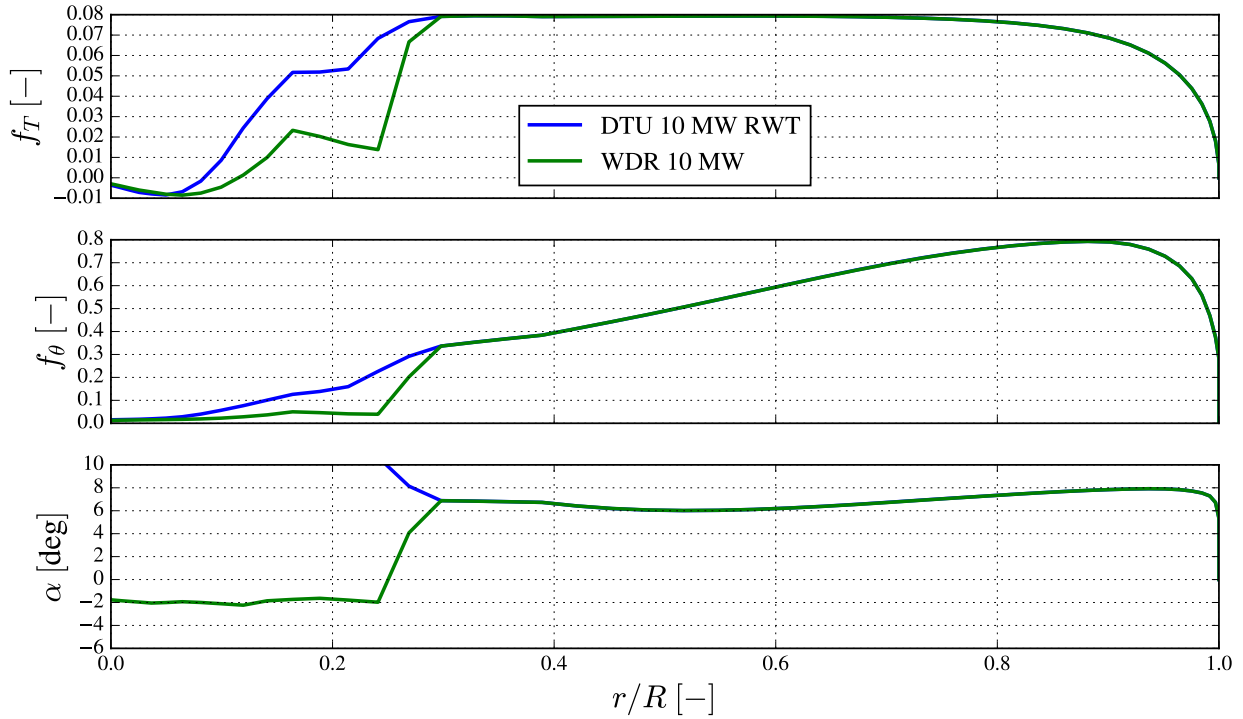


Figure A.3: WDR 10 MW thrust and azimuthal non-dimensionalised force distribution, angle of attack along the blade length.

A.3 Results and Discussion

Figure A.4 shows faster wake velocity deficit recover for the WDR 10 MW design. Analysis of turbulence intensity data depicted in Figure A.5 confirms that the redesign is superior in turbulence generation.

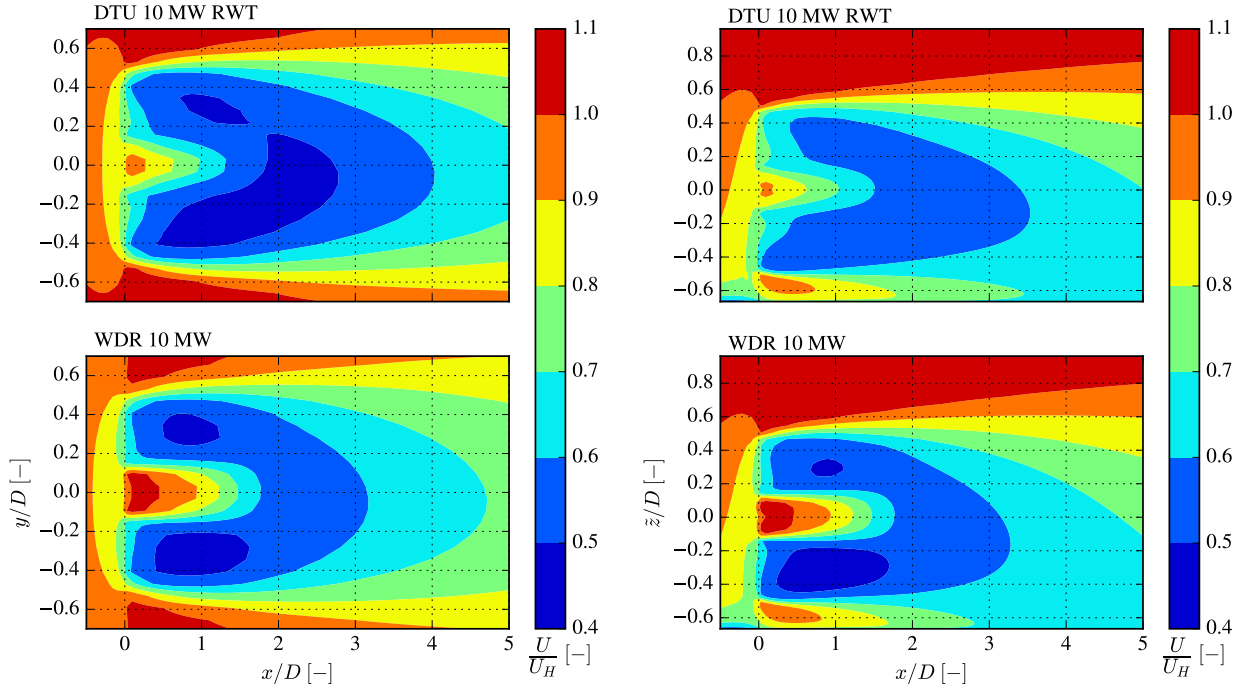


Figure A.4: Velocity deficit contour plots for the DTU 10 MW RWT and WDR 10 MW. Left column: view from the top. Right column: view from the side.

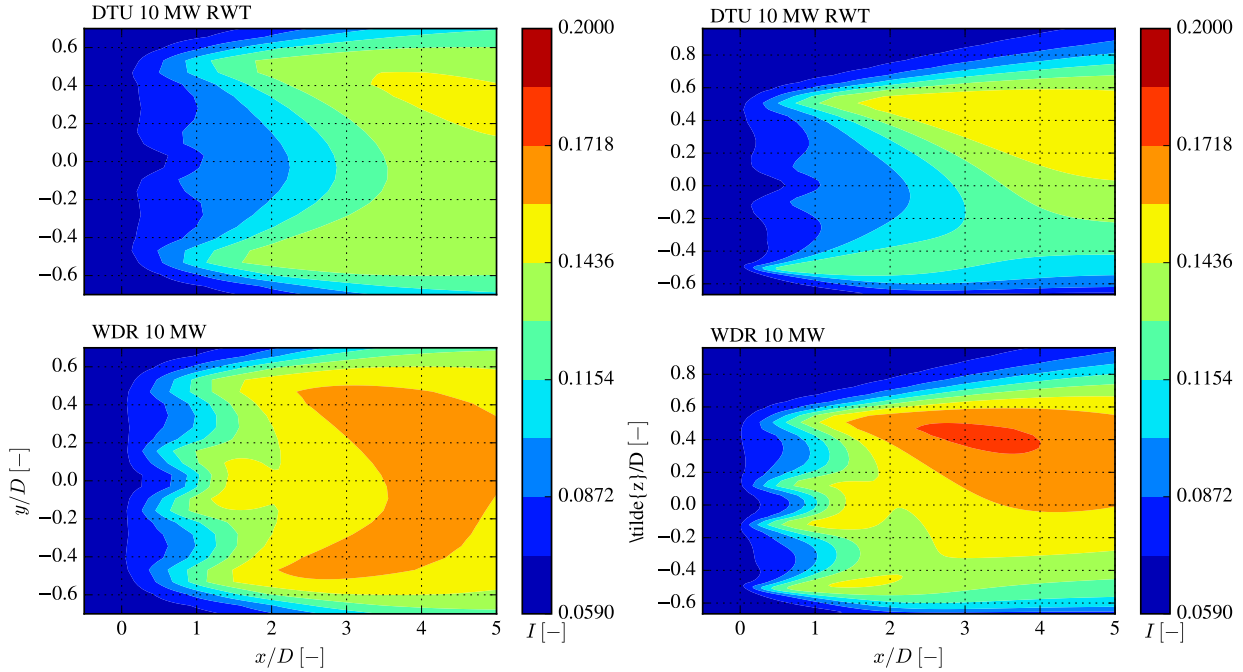


Figure A.5: Turbulence intensity contour plots for the DTU 10 MW RWT and WDR 10 MW. Left column: view from the top. Right column: view from the side.

Both Figures A.6 and A.7 show that the design of WDR 10 MW produces larger Reynolds shear stress gradients in the wake. Using the same method of analysis of momentum transport

as in Subsection 4.1.4, the wake of the WDR 10 MW is found to contain 25 and 27 % more lateral and vertical momentum transfer than the DTU 10 MW RWT - values larger than even the biggest range between $\bar{\delta} = 0.15$ and $\bar{\delta} = 0.60$ for the Joukowsky AD model. This is likely due to the extreme measure of the thrust distribution's reduction near the root for the WDR 10 MW's design.

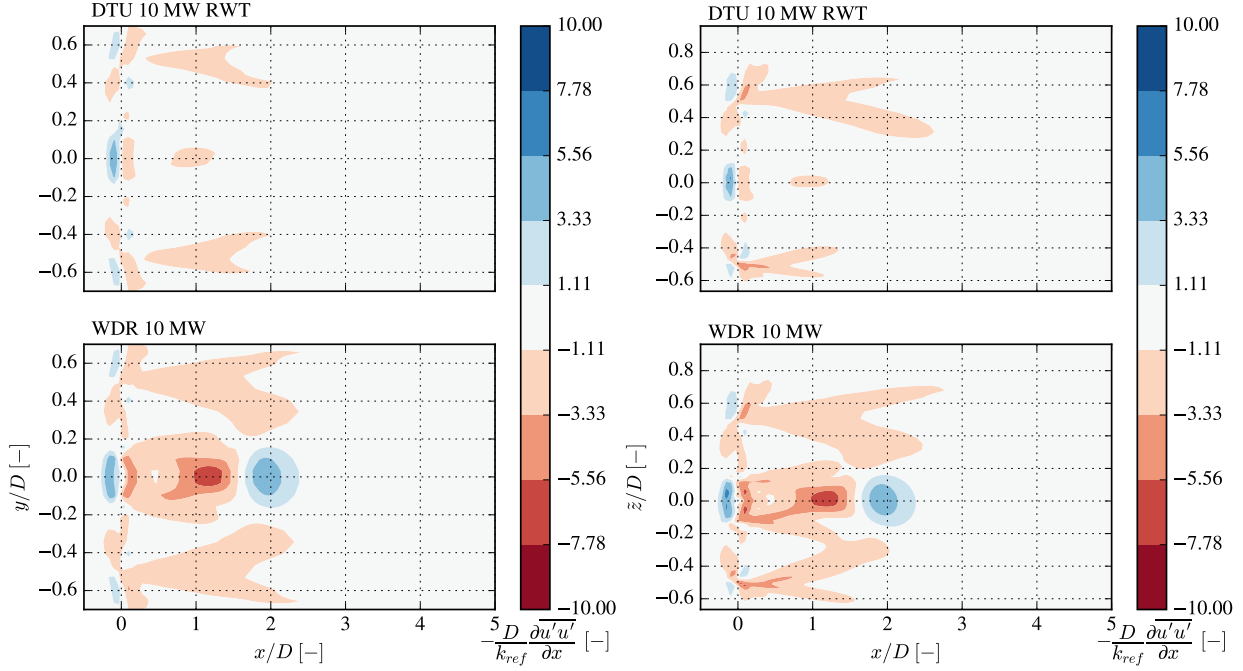


Figure A.6: Streamwise momentum transport term contour plots for the DTU 10 MW RWT and WDR 10 MW. Left column: view from the top. Right column: view from the side.

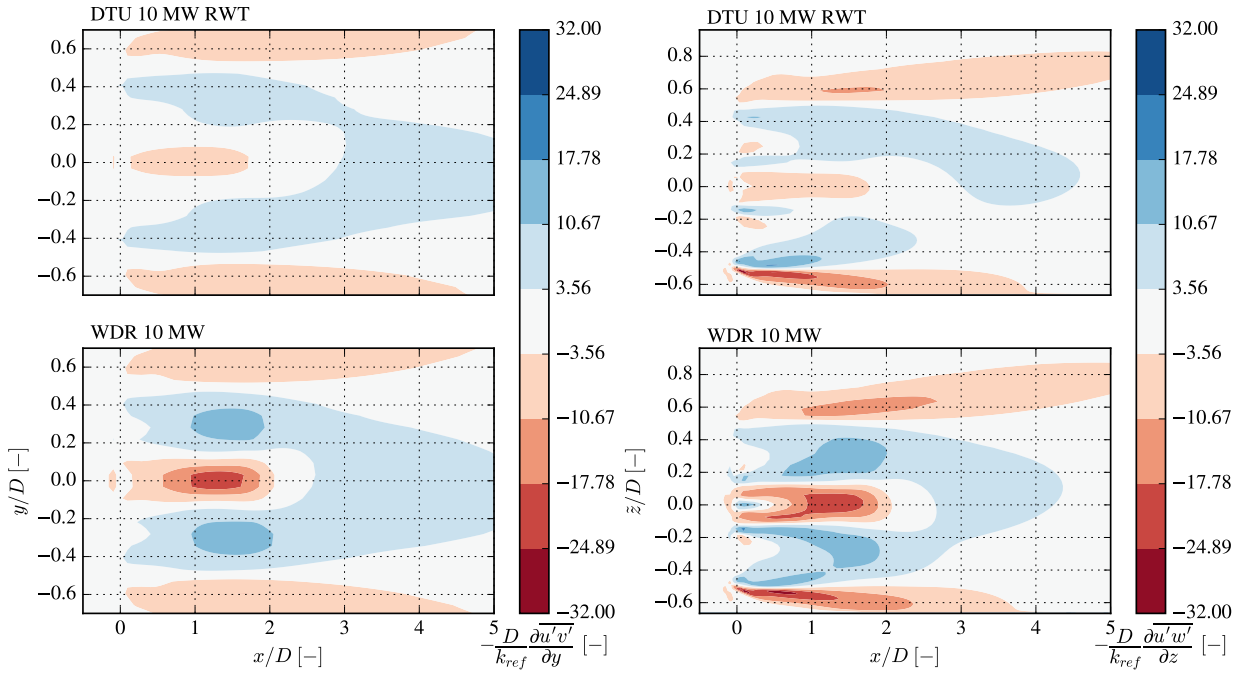


Figure A.7: Momentum transport term contour plots for the DTU 10 MW RWT and WDR 10 MW. Left column: lateral stress gradients, view from the top. Right column: vertical stress gradients, view from the side.

The overall thrust coefficients C_T of the DTU 10 MW RWT and the WDR 10 MW are 0.93 and 0.91 respectively, with a ΔP of -3.4 and -2.7% from HAWC2S and PyWakeEllipSys¹⁴ for the WDR 10 MW compared to the DTU 10 MW RWT. The decrease in the wake velocity deficit $\langle U_{AD} \rangle / U_H$ at $x/D = 5$ of the WDR 10 MW should lead to a roughly 6.3 % gain in possible power capture of the second wind turbine - keep in mind though that this is a gain in power relative to the suboptimal redesign (unless different wind turbine types were used downstream, of course). Simulations of power capture in arrays were not conducted, as the explorative nature of the redesign and its focus neglected overall power optimisation of the wind turbine, both individually and in arrays. Control considerations would need to be taken into account to provide new optimised pitch and rpm curves. Thus, results generated by row studies would hold little strength on which to base conclusions upon without more work, that was already considered outside the scope of the project to begin with.

It should be noted that the overall C_T is not kept as a controlled variable across the two designs, which does lead to a possible conclusion for the accelerated wake recovery effect outside that of the wake-diffusion rotor concept. This other hypothesis would be that the accelerated wake diffusion found for the WDR 10 MW simply stems from the fact that there is less integrated total drag force generated by the redesigned blade. It is difficult to quantify how much this wake-diffusion effect comes from either of these two proposed mechanisms (even though the C_T difference and thus its influence could be argued to be very low), and

¹⁴A difference likely caused by the different implementations of BEM codes in these two software tools, see Section A.1.

thus there is no conclusion made on this case.

However, the analysis of turbulence and Reynolds stress gradients still showed higher generation of turbulence and momentum transport for the redesign. The accelerating effects on wake-diffusion of these aspects are not only confirmed by this study but also present in current literature (see Section 2.1), giving more ground to the feasibility of the wake-diffusion rotor concept.

To re-emphasize, this redesign process was not a systematic, rigorous endeavour, but more of an exploration of the concept examined in this study. Optimisation of power generation for the redesign was not pursued, but rather a confirmation of the wake-diffusing properties of the concepts of 'ventilation' in the inboard rotor section and the thrust distribution in general. This exploration was halted due to being outside the scope of this paper, the time-consuming nature of the iterative design process and its simulations, and the complexity of the task. Good wind turbine design is a difficult endeavour by itself - even without taking the wake into account - and the development of an optimal wake-diffusion rotor remains as a future work suggestion. It is the hope of the author that this Appendix nonetheless provides useful insights both for the understanding of the wake-diffusion rotor concept, and helps anyone interested in pursuing the task of designing such a rotor further.

References

- [1] P. Veers *et al.*, “Grand challenges in the science of wind energy,” *Science*, vol. 366, no. 6464, October 2019. DOI: 10.1126/science.aau2027. [Online]. Available: <https://doi.org/10.1126/science.aau2027>.
- [2] *Dnv’s energy transition outlook 2021*, [Accessed: 29/07/2022]. [Online]. Available: <https://eto.dnv.com/2021>.
- [3] *Offshore wind outlook 2019 – analysis*, [Accessed: 29/07/2022]. [Online]. Available: <https://www.iea.org/reports/offshore-wind-outlook-2019>.
- [4] K. Dykes *et al.*, “Results of ie a wind tcp workshop on a grand vision for wind energy technology,” 2019, Technical Report NREL/TP-5000-72437. [Online]. Available: www.nrel.gov/docs/fy19osti/72437.pdf.
- [5] T. Burton, N. Jenkins, E. Bossanyi, D. Sharpe, and M. Graham, *Wind Energy Handbook*. John Wiley & Sons, 2021, 3rd edition. DOI: 10.1002/9781119451143.
- [6] A. Knauer, “Rotor blade shaped to enhance wake diffusion,” 2016. [Online]. Available: <https://patents.justia.com/patent/10975837>.
- [7] M. O. L. Hansen, “Aerodynamics of wind turbines,” 3rd edition, 2015.
- [8] A. Betz, “Schraubenpropeller mit geringstem energieverlust. mit einem zusatz von l. prandtl. nachrichten von der gesellschaft der wissenschaften zu göttingen,” *Mathematisch-Physikalische Klasse 193-217*, 1919.
- [9] L. J. Vermeer, J. N. Sørensen, and A. Crespo, “Wind turbine wake aerodynamics,” *Progress in Aerospace Sciences*, vol. 39, pp. 467–510, 6-7 2003, ISSN: 03760421. DOI: 10.1016/S0376-0421(03)00078-2.
- [10] A. J. Brand, J. Peinke, and J. Mann, “Turbulence and wind turbines,” *Journal of Physics: Conference series 318*, pp. 409–425, 1 2011. DOI: 10.1088/1742-6596/318/7/072005.
- [11] D. R. Houck, “Review of wake management techniques for wind turbines,” *Wind Energy*, 2021, ISSN: 10991824. DOI: 10.1002/we.2668.
- [12] N. O. Jensen, “A note on wind generator interaction,” Risø National Laboratory, 1983.
- [13] N. Simisiroglou, S. P. Breton, and S. Ivanell, “Validation of the actuator disc approach using small-scale model wind turbines,” *Wind Energy Science*, vol. 2, pp. 587–601, 2 Jul. 2017, ISSN: 23667451. DOI: 10.5194/wes-2-587-2017.
- [14] X. Yang, A. Boomsma, F. Sotiropoulos, B. R. Resor, D. C. Maniaci, and C. L. Kelley, “Effects of spanwise blade load distribution on wind turbine wake evolution,” 2015. DOI: 10.2514/6.2015-0492.

- [15] L. A. Martínez-Tossas *et al.*, “Numerical investigation of wind turbine wakes under high thrust coefficient,” *Wind Energy*, 2021, ISSN: 10991824. DOI: 10.1002/we.2688.
- [16] C. Wang, F. Campagnolo, H. Canet, D. J. Barreiro, and C. L. Bottasso, “How realistic are the wakes of scaled wind turbine models?” *Wind Energy Science*, vol. 6, pp. 961–981, 3 Jun. 2021, ISSN: 23667451. DOI: 10.5194/wes-6-961-2021.
- [17] N. Tobin, A. M. Hamed, and L. P. Chamorro, “An experimental study on the effects of winglets on the wake and performance of a model wind turbine enhanced reader,” *Energies*, vol. 8, 2015, ISSN: 1996-1073. DOI: 10.3390/en81011955.
- [18] V. Klimchenko and A. R. Jones, “An experimental study of the effects of winglets and serrations on the wake of a wind turbine,” American Institute of Aeronautics and Astronautics Inc, AIAA, 2015, ISBN: 9781624103438. DOI: 10.2514/6.2015-1493.
- [19] A. S. Nafi, K. Krishnan, A. K. Debnath, E. E. Hackett, and R. Gurka, “Wake characteristics of a freely rotating bioinspired swept rotor blade,” *Royal Society Open Science*, vol. 8, 7 Jul. 2021, ISSN: 20545703. DOI: 10.1098/rsos.210779.
- [20] J. F. Herbert-Acero, O. Probst, P. E. Réthoré, G. C. Larsen, and K. K. Castillo-Villar, *A review of methodological approaches for the design and optimization of wind farms*, 2014. DOI: 10.3390/en7116930.
- [21] F. Haces-Fernandez, H. Li, and D. Ramirez, “Improving wind farm power output through deactivating selected wind turbines,” *Energy Conversion and Management*, vol. 187, pp. 407–422, May 2019, ISSN: 01968904. DOI: 10.1016/j.enconman.2019.03.028.
- [22] D. R. Houck and E. A. Cowen, “Can you accelerate wind turbine wake decay with unsteady operation?,” American Institute of Aeronautics and Astronautics Inc, AIAA, 2019, ISBN: 9781624105784. DOI: 10.2514/6.2019-2084.
- [23] W. Munters and J. Meyers, “An optimal control framework for dynamic induction control of wind farms and their interaction with the atmospheric boundary layer,” *Philosophical Transactions of the Royal Society A: Mathematical, Physical and Engineering Sciences*, vol. 375, 2091 April 2017, ISSN: 1364503X. DOI: 10.1098/rsta.2016.0100.
- [24] W. Munters and J. Meyers, “Towards practical dynamic induction control of wind farms: Analysis of optimally controlled wind-farm boundary layers and sinusoidal induction control of first-row turbines,” *Wind Energy Science*, vol. 3, pp. 409–425, 1 January 2018, ISSN: 23667451. DOI: 10.5194/wes-3-409-2018.
- [25] C. VerHulst and C. Meneveau, “Altering kinetic energy entrainment in large eddy simulations of large wind farms using unconventional wind turbine actuator forcing,” *Energies*, vol. 8, pp. 370–386, 1 2015, ISSN: 19961073. DOI: 10.3390/en8010370.
- [26] J. Frederik, B. Doekemeijer, S. Mulders, and J. W. V. Wingerden, “On wind farm wake mixing strategies using dynamic individual pitch control,” vol. 1618, IOP Publishing Ltd, Sep. 2020. DOI: 10.1088/1742-6596/1618/2/022050.
- [27] S. H. Bader, V. Inguva, and J. B. Perot, “Improving the efficiency of wind farms via wake manipulation,” *Wind Energy*, vol. 21, pp. 1239–1253, 12 December 2018, ISSN: 10991824. DOI: 10.1002/we.2226.

- [28] N. Johnson *et al.*, “Investigation of innovative rotor concepts for the big adaptive rotor project,” 2019, National Renewable Energy Laboratory, NREL/TP-5000-73605. [Online]. Available: www.nrel.gov/docs/fy19osti/73605.pdf.
- [29] G. K. Suryanarayana, H. Pauer, and G. E. Meier, “Bluff-body drag reduction by passive ventilation,” *Experiments in Fluids*, vol. 16, pp. 73–81, 2 December 1993, ISSN: 07234864. DOI: [10.1007/BF00944909](https://doi.org/10.1007/BF00944909).
- [30] B. G. Newman, “Multiple actuator-disc theory for wind turbines,” 1986, pp. 215–225.
- [31] A. Rosenberg, S. Selvaraj, and A. Sharma, “A novel dual-rotor turbine for increased wind energy capture,” vol. 524, Institute of Physics Publishing, 2014. DOI: [10.1088/1742-6596/524/1/012078](https://doi.org/10.1088/1742-6596/524/1/012078).
- [32] M. P. van der Laan *et al.*, “Power curve and wake analyses of the vestas multi-rotor demonstrator,” *Wind Energy Science*, vol. 4, pp. 251–271, 2 2019, ISSN: 23667451. DOI: [10.5194/wes-4-251-2019](https://doi.org/10.5194/wes-4-251-2019).
- [33] N. S. Ghaisas, A. S. Ghate, and S. K. Lele, “Large-eddy simulation study of multi-rotor wind turbines,” vol. 1037, Institute of Physics Publishing, Jun. 2018. DOI: [10.1088/1742-6596/1037/7/072021](https://doi.org/10.1088/1742-6596/1037/7/072021).
- [34] C. L. Kelley, D. C. Maniaci, and B. R. Resor, “Horizontal-axis wind turbine wake sensitivity to different blade load distributions,” *AIAA*, vol. 5800, 2015. DOI: [10.2514/6.2015-0490](https://doi.org/10.2514/6.2015-0490).
- [35] C. L. Kelley, D. C. Maniaci, and B. R. Resor, “Wind turbine blades, wind turbines, and wind farms having increased power output,” Patent No.: US 10,400,743 B1, 2015.
- [36] B. Moghadassian and A. Sharma, “Designing wind turbine rotor blades to enhance energy capture in turbine arrays,” *Renewable Energy*, vol. 148, pp. 651–664, April 2020, ISSN: 18790682. DOI: [10.1016/j.renene.2019.10.153](https://doi.org/10.1016/j.renene.2019.10.153).
- [37] J. Allen, E. Young, P. Bortolotti, R. King, and G. Barter, “Blade planform design optimization to enhance turbine wake control,” *Wind Energy*, January 2022, ISSN: 1095-4244. DOI: [10.1002/we.2699](https://doi.org/10.1002/we.2699). [Online]. Available: <https://onlinelibrary.wiley.com/doi/10.1002/we.2699>.
- [38] Y. Zhang, V. Ramdoss, Z. Saleem, X. Wang, G. Schepers, and C. Ferreira, “Effects of root gurney flaps on the aerodynamic performance of a horizontal axis wind turbine,” *Energy*, vol. 187, November 2019, ISSN: 03605442. DOI: [10.1016/j.energy.2019.115955](https://doi.org/10.1016/j.energy.2019.115955).
- [39] M. K. McWilliam, T. K. Barlas, H. A. Madsen, and F. Zahle, “Aero-elastic wind turbine design with active flaps for aep maximization,” *Wind Energy Science*, vol. 3, pp. 231–241, 1 January 2018, ISSN: 23667451. DOI: [10.5194/wes-3-231-2018](https://doi.org/10.5194/wes-3-231-2018).
- [40] W. Zhang, Y. Wang, Y. Shen, Y. Wang, Y. Xu, and X. Zhang, “Cfd studies of wake characteristics and power capture of wind turbines with trailing edge flaps,” *IEEE Access*, vol. 8, pp. 7349–7361, 2020, ISSN: 21693536. DOI: [10.1109/ACCESS.2020.2964620](https://doi.org/10.1109/ACCESS.2020.2964620).
- [41] G. A. Speakman, M. Abkar, L. A. Martínez-Tossas, and M. Bastankhah, “Wake steering of multirotor wind turbines,” *Wind Energy*, vol. 24, pp. 1294–1314, 11 November 2021, ISSN: 10991824. DOI: [10.1002/we.2633](https://doi.org/10.1002/we.2633).

- [42] A. P. Stanley and A. Ning, “Coupled wind turbine design and layout optimization with nonhomogeneous wind turbines,” *Wind Energy Science*, vol. 4, pp. 99–114, 1 January 2019, ISSN: 23667451. DOI: 10.5194/wes-4-99-2019.
- [43] N. N. Sørensen, “General purpose flow solver applied to flow over hills,” 1995, Risø-R-827(EN).
- [44] J. A. Michelsen, “Basis 3d — a platform for development of multiblock pde solvers,” 1992, Technical Report AFM 92-05.
- [45] M. P. van der Laan *et al.*, “An improved $k-\varepsilon$ model applied to a wind turbine wake in atmospheric turbulence,” *Wind Energy*, vol. 18, pp. 889–907, 5 May 2015, ISSN: 10991824. DOI: 10.1002/we.1736.
- [46] J. Boussinesq, “Essai sur la théorie des eaux courantes,” 1887, Mémoires présentés par divers savants à l’Académie des Sciences 23 (1): 1-680.
- [47] M. P. van der Laan and S. J. Andersen, “The turbulence scales of a wind turbine wake: A revisit of extended k -epsilon models,” vol. 1037, Institute of Physics Publishing, Jun. 2018. DOI: 10.1088/1742-6596/1037/7/072001.
- [48] P.-E. Réthoré, M. P. van der Laan, N. Troldborg, F. Zahle, and N. N. Sørensen, “Verification and validation of an actuator disc model,” *Wind Energy*, vol. 17, pp. 919–937, 6 2014, ISSN: 10991824. DOI: 10.1002/we.1607.
- [49] N. Troldborg, N. N. Sørensen, P. E. Réthoré, and M. P. van der Laan, “A consistent method for finite volume discretization of body forces on collocated grids applied to flow through an actuator disk,” *Computers and Fluids*, vol. 119, pp. 197–203, Sep. 2015, ISSN: 00457930. DOI: 10.1016/j.compfluid.2015.06.028.
- [50] J. N. Sørensen, K. Nilsson, S. Ivanell, H. Asmuth, and R. F. Mikkelsen, “Analytical body forces in numerical actuator disc model of wind turbines,” *Renewable Energy*, vol. 147, pp. 2259–2271, March 2020, ISSN: 18790682. DOI: 10.1016/j.renene.2019.09.134.
- [51] M. P. van der Laan *et al.*, “The $k-\varepsilon-f_P$ model applied to wind farms,” *Wind Energy*, pp. 2065–2084, 18 2015. DOI: 10.1002/we.1804.
- [52] M. P. van der Laan, S. J. Andersen, and P. E. Réthoré, “Brief communication: Wind-speed-independent actuator disk control for faster annual energy production calculations of wind farms using computational fluid dynamics,” *Wind Energy Science*, vol. 4, pp. 645–651, 4 December 2019, ISSN: 23667451. DOI: 10.5194/wes-4-645-2019.
- [53] C. Bak *et al.*, “Description of the dtu 10 mw reference wind turbine,” 2013, DTU - Department of Wind Energy Report I-0092.
- [54] J. Jonkman, S. Butterfield, W. Musial, and G. Scott, “Definition of a 5-mw reference wind turbine for offshore system development,” 2009, Technical Report NREL/TP-500-38060.
- [55] M. Baungaard, M. P. van der Laan, and M. Kelly, “Rans modelling of a single wind turbine wake in the unstable surface layer,” *Wind Energy Science*, vol. 7, pp. 783–800, 2022. DOI: 10.5194/wes-2021-94.
- [56] M. C. Baungaard, “Modeling of aerodynamic rotor interaction for multi-rotor wind turbines,” Jul. 2019, DTU Wind Energy-M-0271, MSc Thesis.

- [57] I. Troen and E. L. Petersen, “European wind atlas,” Risø National Laboratory, 1989.
- [58] R. Stull, “Meteorology for scientists & engineers,” 3rd edition, 2017, Univ. of British Columbia. isbn 978-0-88865-178-5.
- [59] S. Ivanell, R. Mikkelsen, J. N. Sørensen, and D. Henningson, “Stability analysis of the tip vortices of a wind turbine,” *Wind Energy*, vol. 13, pp. 705–715, 8 2010, ISSN: 10991824. DOI: [10.1002/we.391](https://doi.org/10.1002/we.391).
- [60] M. P. van der Laan, M. Baungaard, and M. Kelly, “Brief communication: A clarification of wake recovery mechanisms,” Technical University of Denmark, DTU Wind Energy, 2022. DOI: [10.5194/wes-2022-56](https://doi.org/10.5194/wes-2022-56).
- [61] M. P. van der Laan and M. Abkar, “Improved energy production of multi-rotor wind farms,” vol. 1256, Institute of Physics Publishing, Jul. 2019. DOI: [10.1088/1742-6596/1256/1/012011](https://doi.org/10.1088/1742-6596/1256/1/012011).